Dynamic analysis of Pine Flat dam-reservoir system utilizing Hagstrom-Warburton truncation boundary condition

Solmaz Dehghanmarvasty[a] and Vahid Lotfi[*]

Department of Civil and Environmental Engineering, Amirkabir University of Technology, Tehran, Iran

Abstract. Dynamic analysis of a typical concrete gravity dam-reservoir system is formulated by FE-(FE-TE) approach (i.e., Finite Element-(Finite Element-Truncation Element)). In this technique, dam and reservoir are discretized by plane solid and fluid finite elements. Moreover, the H-W (i.e., Hagstrom-Warburton) high-order condition imposed at the reservoir truncation boundary. This task is formulated by employing a truncation element at that boundary. It is emphasized that reservoir far-field is excluded from the discretized model. The formulation is initially reviewed which was originally proposed in a previous study. Thereafter, the response of Pine Flat dam-reservoir system is studied due to horizontal and vertical ground motions for two types of reservoir bottom conditions of full reflective and absorptive. It should be emphasized that study is carried out under high order of H-W condition applied on the truncation boundary. The initial part of study is focused on the time harmonic analysis. In this part, it is possible to compare the transfer functions against corresponding responses obtained by FE-(FE-HE) approach (referred to as exact method). Subsequently, the transient analysis is carried out. In that part, it is only possible to compare the results for low and high normalized reservoir length cases. Therefore, the sensitivity of results is controlled due to normalized reservoir length values.

Keywords: absorbing boundary conditions; Hagstrom-Warburton condition; high-order condition; Pine Flat dam; truncation boundary

1. Introduction

In general, fluid-structure interaction is still an active research (Hadzalic *et al.* 2018, 2019). Moreover, there has been extensive research about dynamic analysis of concrete gravity dam-reservoir systems in particular. This was mainly carried out by the rigorous FE-(FE-HE) (i.e., Finite Element-(Finite Element-Hyper Element)) method in the frequency domain. This means that the dam is discretized by plane solid finite elements, while, the reservoir is divided into two parts, a near-field region (usually an irregular shape) in the vicinity of the dam and a far-field part (assuming constant depth) which extends to infinity in the upstream direction. The former region is discretized by fluid finite elements and the latter part is modeled by a two-dimensional fluid hyper-element (Hall and Chopra 1982, Waas 1972). It is also understood that employing fluid

---

*Corresponding author, Professor, E-mail: vahlotfi@aut.ac.ir
[a]Ph.D. Candidate

hyper-element would lead to the exact solution (in numerical sense) of the problem. However, it is formulated in the frequency domain and its application in this field has led to many especial purpose programs which were demanding from programming point of view.

On the other hand, engineers have often tried to solve this problem in the context of pure finite element programming (FE-FE method of analysis). In this approach, an often simplified condition is imposed on the truncation boundary or the upstream face of the near-field water domain. Thus, the fluid hyper-element is actually excluded from the model. One of these widely used methods is based on Sommerfeld truncation boundary condition (Sommerfeld 1949). The main advantage of this condition is that it can be readily used for time domain analysis. Thus, they are also vastly employed in nonlinear seismic analysis of concrete dams (Lokke and Chopra 2017, Lokke and Chopra 2018). However, its major shortcoming is that the results have significant errors when low normalized reservoir lengths are utilized (Lotfi and Zenz 2016, Lotfi and Zenz 2018). Moreover, there are also many studies which have employed Westergaard approach for seismic analysis of concrete dams to simplify dam-reservoir interaction even further (Karabulut and Kartal 2018, Lotfi and Omidi 2012).

Of course, there have also been many researches in the last three decades to develop more accurate absorbing boundary conditions to be applied for similar fluid-structure or soil-structure interaction problems. It should be emphasized that many of these studies are actually limited their works to two-dimensional cases. Perfectly matched layer (Berenger 1994, Chew and Weedon 1994, Basu and Chopra 2003, Jiong *et al.* 2009, Zhen *et al.* 2009, Kim and Pasciak 2012, Khazaee and Lotfi 2014a, Khazaee and Lotfi 2014b) and, high-order non-reflecting boundary condition (Higdon 1986, Givoli and Neta 2003, Hagstrom and Warburton 2004, Givoli, *et al.* 2006, Hagstrom *et al.* 2008, Rabinovich *et al.* 2011, Samii and Lotfi 2012) are among the two main popular groups of methods which researchers have applied in their attempts. It is emphasized that these techniques have become very popular in recent years due to the fact that they could be applied in time domain as well as the frequency domain.

Furthermore, the Wavenumber approach was introduced in 2012 based on the FE method. Initially, this approach was introduced just for horizontal ground excitation and full reflective reservoir base condition (Lotfi and Samii, 2012). Later on, some modifications were implemented to expand the technique for general reservoir base condition (Jafari and Lotfi, 2017). Subsequently, it was discussed for the general reservoir base condition and ground excitation (Lotfi, 2017).

The present study formulation is based on FE-(FE-TE) (i.e., Finite Element-(Finite Element-Truncation Element)) procedure for dynamic analysis of concrete gravity dam-reservoir systems. The formulation is initially reviewed which was originally proposed in a previous study (Dehghanmarvasty and Lotfi 2022). It should be emphasized that the core of the method is based on utilizing a truncation-element at the U/S (i.e., Upstream) truncation boundary of the reservoir near-field domain and excluding far-field region of the reservoir. This truncation-element is formulated based on the H-W type (i.e., Hagstrom-Warburton) high-order condition applied at that boundary (Hagstrom and Warburton 2004, Hagstrom *et al.* 2008). Moreover, a special purpose finite element program (Lotfi 2001a) is enhanced for this investigation based on the explained formulation. Thereafter, the response of Pine Flat dam-reservoir system is studied due to horizontal and vertical ground motions. Furthermore, two conditions of full reflective and absorptive reservoir bottom are considered.

The initial part of study is focused on the time harmonic analysis. In this part, it is possible to compare the transfer functions against corresponding responses obtained by rigorous FE-(FE-HE)

approach (referred to as exact method). Subsequently, the transient analysis is carried out. In this part, it is only possible to compare the results for low and high normalized reservoir length cases. Therefore, the sensitivity of results is controlled due to normalized reservoir length values.

Finally, it needs to be emphasized that in the case of high-order non-reflecting boundary condition which is the core of the present work, one can encounter stability problems in certain cases such as the G-N approach (Givoli and Neta 2003, Givoli *et al.* 2006). Of course, this is mainly occurring when very high orders are utilized (Lotfi and Lotfi 2022, Dehghanmarvasty and Lotfi 2023). Fortunately, this problem was later resolved through H-W formulation (Hagstrom and Warburton 2004, Hagstrom *et al.* 2008) and this is the main reason for employing this approach in the present study.

2. Method of analysis

As mentioned, the analysis technique utilized in this study is based on the FE-(FE-TE) method, which is applicable for a general concrete gravity dam-reservoir system. The formulation is described in great details in the previous study (Dehghanmarvasty and Lotfi 2022). However, the salient aspects of the approach will be reviewed in this section.

For this aim, let us consider a concrete gravity dam-reservoir system. The coupled equations can be obtained by considering each region separately and then combine the resulting equations.

2.1 Dam body

Concentrating on the structural part, the dynamic behavior of the dam is described by the well-known equation of structural dynamics (Zienkiewicz and Taylor 2000)

$$\mathbf{M}\,\ddot{\mathbf{r}} + \mathbf{C}\,\dot{\mathbf{r}} + \mathbf{K}\,\mathbf{r} = -\widetilde{\mathbf{M}}\,\mathbf{J}\,\mathbf{a}_g + \mathbf{B}^{\mathrm{T}}\mathbf{P} \tag{1}$$

where $\mathbf{M}$, $\mathbf{C}$ and $\mathbf{K}$ in this relation represent mass, damping and stiffness matrices of the dam body. Moreover, $\mathbf{r}$ is the vector of nodal relative displacements, $\widetilde{\mathbf{M}}$ is the same as $\mathbf{M}$ matrix except that no columns are excluded due to restraints, $\mathbf{J}$ is a matrix with each two rows equal to a 2×2 identity matrix (its columns correspond to a unit horizontal and vertical rigid body motion) and $\mathbf{a}_g$ denotes the vector of ground accelerations. Furthermore, $\mathbf{B}$ is a matrix which relates vectors of hydrodynamic pressures (i.e., $\mathbf{P}$), and its equivalent nodal forces. It should be also emphasized that $\mathbf{a}_g$ denotes the vector of ground accelerations in two directions.

2.2 Water domain

Assuming water to be linearly compressible and neglecting its viscosity, its small irrotational motion (Fig. 1) is governed by the wave equation (Chopra 1967, Chopra *et al.* 1980)

$$\nabla^2 P - \frac{1}{c^2}\ddot{P} = 0 \; ; \qquad\qquad \text{in } \Omega \text{ and } D \tag{2}$$

where P is the hydrodynamic pressure and, c is the pressure wave velocity in water. Apart from truncation boundary condition for upstream face of the water domain (Γ_{I}) which is discussed on subsequent sections, the boundary conditions for water domain are as follows:

$$\partial_n P = -\rho a_g^n - q\dot{P} \; ; \qquad\qquad \text{at reservoir's bottom } (\Gamma_{\mathrm{II}}) \tag{3a}$$

$$\partial_n P = -\rho \, \ddot{u}_n \; ; \qquad \text{at dam-water interface } (\Gamma_{\text{III}}) \qquad (3b)$$

$$P = 0 \; ; \text{ on water surface } (\Gamma_{\text{IV}}) \qquad (3c)$$

Herein, ρ is the water density and n denotes the outward perpendicular direction (with respect to fluid region) and $\ddot{u}_n$ is the normal acceleration of fluid particles at dam-reservoir interface which is equal to solid particle total acceleration in that direction due to compatibility of acceleration. It should be also emphasized that $\partial_n P$ refers to partial derivative of P with respect to n-direction (i.e, $\partial_n P = \partial P / \partial n$). Moreover, the admittance or damping coefficient q utilized in Eq. (3a), may be related to a more meaningful wave reflection coefficient α (Fenves and Chopra 1985)

$$\alpha = \frac{1-qc}{1+qc} \qquad (4)$$

which is defined as the ratio of the amplitude of reflected hydrodynamic pressure wave to the amplitude of incident pressure wave normal to the reservoir's bottom. For a fully reflective reservoir's bottom condition, α is equal to 1 which leads to $q = 0$.

One can apply the weighted residual approach to obtain the finite element equation of the fluid domain, which may be written as

$$\mathbf{G} \, \ddot{\mathbf{P}} + q \, \mathbf{L}_{\text{II}}\dot{\mathbf{P}} + \mathbf{H} \, \mathbf{P} = \mathbf{R}_{\text{I}} - \mathbf{B} \, \ddot{\mathbf{r}} - \widetilde{\mathbf{B}} \, \mathbf{J} \, \mathbf{a}_{\text{g}} \qquad (5)$$

In this relation, $\mathbf{G}$, $\mathbf{H}$ are fluid domain's generalized mass and stiffness matrices and $\mathbf{P}$ is the vector of nodal pressures. It should be emphasized that all boundary conditions are already considered in Eq. (5). In particular, the ones related to reservoir bottom's surface (i.e., Γ_{II}; (Fig. 1)) through $\mathbf{L}_{\text{II}}$ matrix, water surface, and the contribution related to the truncation boundary condition is symbolically denoted by the vector $\mathbf{R}_{\text{I}}$. Furthermore, matrix $\mathbf{B}$, is resulted due to dam-reservoir boundary condition (i.e., Γ_{III}), which also appears in Eq. (1). Matrix $\widetilde{\mathbf{B}}$ is the same as matrix $\mathbf{B}$ except that no columns are excluded due to restraints, and it has contributions due to reservoir bottom, as well as dam-reservoir's interface.

It is also worthwhile to emphasize that $\mathbf{R}_{\text{I}}$ is obtained by assembling the following boundary integrals of the fluid elements adjacent to that surface (i.e., Γ_{I})

$$\mathbf{R}^e = \frac{1}{\rho} \int_{\Gamma^e} \mathbf{N} \, (\partial_n P) d\Gamma^e \qquad (6)$$

With $\mathbf{N}$ being the vector of element's shape functions and n denotes the fluid element's outward normal direction.

2.3 Dam-reservoir system

The necessary equations for both dam and reservoir domains were explained in previous sections. Thus, combining the main relations (1) and (5) would result in the FE equations of the coupled dam-reservoir system in its initial form for the time domain

$$\begin{pmatrix} \mathbf{M} & \mathbf{0} \\ \mathbf{B} & \mathbf{G} \end{pmatrix}\begin{pmatrix} \ddot{\mathbf{r}} \\ \ddot{\mathbf{P}} \end{pmatrix} + \begin{pmatrix} \mathbf{C} & \mathbf{0} \\ \mathbf{0} & q\mathbf{L}_{\text{II}} \end{pmatrix}\begin{pmatrix} \dot{\mathbf{r}} \\ \dot{\mathbf{P}} \end{pmatrix} + \begin{pmatrix} \mathbf{K} & -\mathbf{B}^{\text{T}} \\ \mathbf{0} & \mathbf{H} \end{pmatrix}\begin{pmatrix} \mathbf{r} \\ \mathbf{P} \end{pmatrix} + \begin{pmatrix} \mathbf{0} \\ -\mathbf{R}_{\text{I}} \end{pmatrix} = \begin{pmatrix} -\widetilde{\mathbf{M}} \, \mathbf{J} \, \mathbf{a}_{\text{g}} \\ -\widetilde{\mathbf{B}} \, \mathbf{J} \, \mathbf{a}_{\text{g}} \end{pmatrix} \qquad (7)$$

It is noted from the above equation that vector $\mathbf{R}_{\text{I}}$ still needs to be defined by some appropriate condition. This is related to the truncated boundary Γ_{I}. It is interesting to note that one may presume that there exists a truncation-element attached at this boundary similar to hyper-element
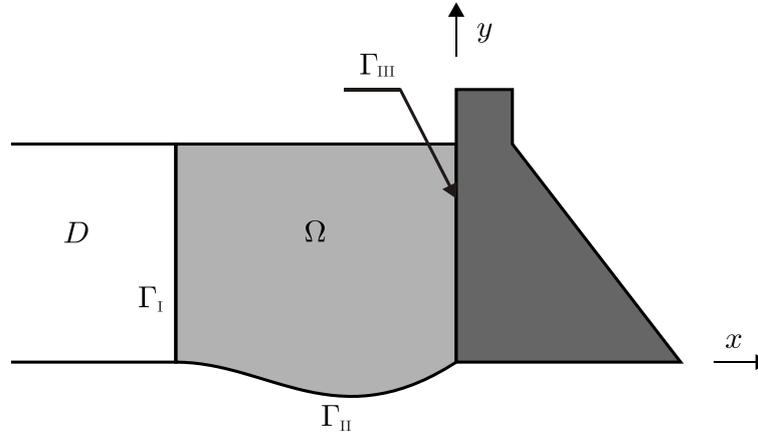
Fig. 1 Schematic view of a typical dam-reservoir system. The near-field reservoir domain Ω, the truncation boundary Γ_I and the far-field region D

role in FE-(FE-HE) approach. The purpose of this element is to generate the vector $\mathbf{R}_I$ based on H-W high-order truncation boundary condition. The element will have generalized mass, damping and stiffness matrices similar to usual solid or fluid finite elements. The details will be discussed below.

2.4 Definition of R_I vector for general excitations

The effect of truncation boundary condition will be treated in this section. For this purpose, let us now assume that the truncation boundary (i.e., Γ_I) is vertical (i.e., along y-direction, Fig. 1). It is apparent that $\mathbf{R}_I$ vector is obtained by assemblage of contributions from different fluid finite elements (i.e., $\mathbf{R}_I^e$). For this aim, one may utilize Eq. (6) to obtain $\mathbf{R}_I^e$, if there is merely horizontal excitation. However, the following equation must be employed in general condition that vertical excitation may also exist

$$\mathbf{R}_I^e = \frac{1}{\rho} \int_{\Gamma_I^e} \mathbf{N} \, (\partial_n P^s) d\Gamma^e \tag{8}$$

It should be emphasized that $\partial_n P^s$ refers to partial derivative of P^s with respect to n-direction (i.e, $\partial_n P^s = \partial P^s / \partial n$). Moreover, it is noted that P^s (scattered pressure) term is substituted for P (total pressure), and they are related as follows

$$P^s = P - P^i \tag{9}$$

The P^i is the incidence pressure contribution which is due to ground acceleration imposed at bottom of uniform part extending to infinity in the upstream direction (Fig. 1). It is noted that this is actually eliminated in our current discretization since it is beyond the truncation boundary. However, incidence pressure's effect is included in the present approach through relations (8) and (9).

Let us also now substitute P^s by another function ϕ_0 which is utilized in writing the H-W high-order boundary condition later on

$$\phi_0 = P^s \tag{10}$$

Employing this function, relation (8) may be rewritten as follows

$$\mathbf{R}_I^e = \frac{1}{\rho} \int_{\Gamma_I^e} \mathbf{N} \, (-\partial_x \phi_0) d\Gamma^e \tag{11}$$

It is noted that negative sign in this relation is due to the fact that the outward normal is opposite to the x-direction for fluid finite elements adjacent to the truncation boundary (Fig. 1). It is obvious that simplified relations (e.g., Sommerfeld condition) may be utilized in relation (11) to explicitly define that vector. However, that would not produce accurate results for low values of normalized reservoir length as previously mentioned. This is due to the fact that Sommerfeld condition is merely designed for incident-wave propagating normal to the truncation boundary and it is not appropriate for inclined incident waves. Therefore, one would prefer to resort to high-order conditions as presented in the next section.

3. H-W type truncation-element

3.1 Extraction of basic relations

As mentioned, high-order conditions are adopted herein for the truncation boundary. In particular, H-W condition is employed in the present study. This condition was initially proposed to absorb propagating waves at the applied boundary (Hagstrom and Warburton 2004) through N-terms. However, it was later generalized to include also evanescent waves (Hagstrom *et al.* 2008) through additional M-terms. Accordingly, one can write the H-W condition of order N, M+1 (i.e., ON-(M+1)) as follows for the truncation boundary

$$\partial_t \phi_1 = (a_0 \partial_t - c \partial_x) \phi_0 \tag{12a}$$

$$\left(a_j \partial_t + c \partial_x \right) \phi_{j+1} = \left(a_j \partial_t - c \partial_x \right) \phi_j \qquad ; \quad j = 1, \dots, N \tag{12b}$$

$$\left(b_j + c \partial_x \right) \phi_{N+j+1} = \left(b_j - c \partial_x \right) \phi_{N+j} \qquad ; \quad j = 1, \dots, M \tag{12c}$$

$$\phi_{N+M+1} = 0 \tag{12d}$$

It is worthwhile to emphasize that common partial derivative abbreviations are utilized in the above relations (i.e., $\partial_t (*) = \partial(*)/\partial t$ and $\partial_x (*) = \partial(*)/\partial x$). Eqs. (12a-d) may alternatively be written in a more simplified form

$$\bar{c} \partial_t \phi_1 = (\bar{a}_0 \partial_t - \partial_x) \phi_0 \tag{13a}$$

$$\left(\bar{a}_j \partial_t + \partial_x \right) \phi_{j+1} = \left(\bar{a}_j \partial_t - \partial_x \right) \phi_j \qquad ; \quad j = 1, \dots, N \tag{13b}$$

$$\left(\bar{b}_j + \partial_x \right) \phi_{N+j+1} = \left(\bar{b}_j - \partial_x \right) \phi_{N+j} \qquad ; \quad j = 1, \dots, M \tag{13c}$$

$$\phi_{N+M+1} = 0 \tag{13d}$$

With the following definitions for normalized coefficients $\bar{a}_j$, $\bar{b}_j$ and $\bar{c}$

$$\bar{a}_j = \frac{a_j}{c} \quad ; \quad j = 1, \dots, N \tag{14a}$$

$$\bar{b}_j = \frac{b_j}{c} \quad ; \quad j = 1, \dots, M \tag{14b}$$

$$\bar{c} = \frac{1}{c} \tag{14c}$$

In which c is the pressure wave velocity of fluid. It is recalled that ϕ_0 is the same as function P^s (scattered pressure wave) which itself should satisfy the governing wave equation in fluid domain. Therefore, all auxiliary functions ϕ_j would also satisfy similar equation, since they are related through a given set of operators

$$\nabla^2 \phi_j = \bar{c}^2 \ddot{\phi}_j \tag{15}$$

Moreover, these auxiliary functions should satisfy boundary conditions at reservoir bottom similar to ϕ_0

$$\partial_y \phi_j = q \, \partial_t \phi_j \tag{16}$$

It is worthwhile to emphasize that admittance coefficient q is related to reflection coefficient α through Eq. (4).

By applying certain operators to Eq. (13a), Eq. (13b) for $j = 1$ and combining them, the result may be written as (Dehghanmarvasty and Lotfi 2022)

$$(2\bar{a}_1/\bar{c}) \left[(\bar{a}_0^2 - \bar{c}^2)\partial_t^2 + \partial_y^2 \right]\phi_0 + \left[-(2\bar{a}_0\bar{a}_1 + \bar{a}_1^2 + \bar{c}^2)\partial_t^2 + \partial_y^2 \right]\phi_1$$
$$+ \left[(\bar{a}_1^2 - \bar{c}^2)\partial_t^2 + \partial_y^2 \right]\phi_2 = 0 \tag{17}$$

Similarly, apply appropriate operators to Eq. (13b) for $j - 1$ and j and combining them, the following relation is obtained

$$\bar{a}_j \left[(\bar{a}_{j-1}^2 - \bar{c}^2)\partial_t^2 + \partial_y^2 \right]\phi_{j-1} + \bar{a}_j \left[-(\bar{a}_{j-1}^2 + \bar{c}^2)\partial_t^2 + \partial_y^2 \right]\phi_j + \bar{a}_{j-1}\left[-(\bar{a}_j^2 + \bar{c}^2)\partial_t^2 + \right.$$
$$\left. \partial_y^2 \right]\phi_j + \bar{a}_{j-1}\left[(\bar{a}_j^2 - \bar{c}^2)\partial_t^2 + \partial_y^2 \right]\phi_{j+1} = 0 \tag{18}$$

Thereafter, apply similar operators to Eq. (13b) for $j = N$ and Eq. (13c) for $j = 1$ which may be written as

$$\left[(\bar{a}_N^2 - \bar{c}^2)\partial_t^2 + \partial_y^2 \right]\phi_N + \left[-(\bar{a}_N^2 + \bar{c}^2)\partial_t^2 + \partial_y^2 \right]\phi_{N+1} - 2\bar{a}_N\partial_t\psi = 0 \tag{19}$$

$$\left[-\bar{b}_1^2 - \bar{c}^2\partial_t^2 + \partial_y^2 \right]\phi_{N+1} + \left[\bar{b}_1^2 - \bar{c}^2\partial_t^2 + \partial_y^2 \right]\phi_{N+2} + 2\bar{b}_1\psi = 0 \tag{20}$$

By invoking the following auxiliary function

$$\psi = \partial_x \phi_{N+1} \tag{21}$$

The above process continues by employing Eq. (13c) for j and $j + 1$ and combining them which leads to the following relation

$$\bar{b}_{j+1}\left[\bar{b}_j^2 - \bar{c}^2\partial_t^2 + \partial_y^2 \right]\phi_{N+j} + \bar{b}_{j+1}\left[-\bar{b}_j^2 - \bar{c}^2\partial_t^2 + \partial_y^2 \right]\phi_{N+j+1} + \bar{b}_j\left[-\bar{b}_{j+1}^2 - \bar{c}^2\partial_t^2 + \right.$$
$$\left. \partial_y^2 \right]\phi_{N+j+1} + \bar{b}_j\left[\bar{b}_{j+1}^2 - \bar{c}^2\partial_t^2 + \partial_y^2 \right]\phi_{N+j+2} = 0 \tag{22}$$

Let us now apply weighted residual approach on obtained relations (Eqs (17)-(20), and Eq. (22)) by multiplying them with a weighting function w and integrate them on the truncation boundary for each fluid finite element as follows

$$-\frac{1}{\rho}\int_y w\left[(2\bar{a}_1/\bar{c})\alpha_0\ddot{\phi}_0 - (2\bar{a}_0\bar{a}_1 + \beta_1)\ddot{\phi}_1 + \alpha_1\ddot{\phi}_2 + \partial_y^2 \left((2\bar{a}_1/\bar{c})\phi_0 + \phi_1 + \phi_2 \right) \right] dy = 0 \tag{23a}$$

$$-\frac{1}{\rho}\int_y w\left[\bar{a}_j\alpha_{j-1}\ddot{\phi}_{j-1} - \gamma_j\ddot{\phi}_j + \bar{a}_{j-1}\alpha_j\ddot{\phi}_{j+1} + \partial_y^2 \left(\bar{a}_j\phi_{j-1} + \xi_{j-1}\phi_j + \bar{a}_{j-1}\phi_{j+1} \right) \right] dy = 0 \tag{23b}$$

$$-\frac{1}{\rho}\int_y w\left[\alpha_N\ddot{\phi}_N - \beta_N\ddot{\phi}_{N+1} - 2\bar{a}_N\dot{\psi} + \partial_y^2 \left(\phi_N + \phi_{N+1} \right) \right] dy = 0 \tag{23c}$$

$$-\frac{1}{\rho}\int_y w\left[-\bar{c}^2\ddot{\phi}_{N+1} - \bar{c}^2\ddot{\phi}_{N+2} + 2\bar{b}_1\psi - \bar{b}_1^2\phi_{N+1} + \bar{b}_1^2\phi_{N+2} + \partial_y^2(\phi_{N+1} + \phi_{N+2})\right]dy = 0 \tag{23d}$$

$$-\frac{1}{\rho}\int_y w\left[-\bar{b}_{j+1}\bar{c}^2\ddot{\phi}_{N+j} - \eta_j\bar{c}^2\ddot{\phi}_{N+j+1} - \bar{b}_j\bar{c}^2\ddot{\phi}_{N+j+2} + \bar{b}_{j+1}\bar{b}_j^2\phi_{N+j} - \\ \bar{b}_j\bar{b}_{j+1}\eta_j\phi_{N+j+1} + \bar{b}_j\bar{b}_{j+1}^2\phi_{N+j+2} + \partial_y^2\left(+\bar{b}_{j+1}\phi_{N+j} + \eta_j\phi_{N+j+1} + \bar{b}_j\phi_{N+j+2}\right)\right]dy = 0 \tag{23e}$$

It is noticed that certain simplifying parameters are also employed in these relations, which are defined as

$$\xi_j = \bar{a}_j + \bar{a}_{j+1} \quad ; j = 1, \ldots\ldots, N-1 \tag{24a}$$

$$\eta_j = \bar{b}_j + \bar{b}_{j+1} \quad ; j = 1, \ldots\ldots, M-1 \tag{24b}$$

$$\alpha_j = \bar{a}_j^2 - \bar{c}^2 \quad ; j = 0, \ldots\ldots, N \tag{24c}$$

$$\beta_j = \bar{a}_j^2 + \bar{c}^2 \quad ; j = 1, \ldots\ldots, N \tag{24d}$$

$$\gamma_j = \bar{a}_j\beta_{j-1} + \bar{a}_{j-1}\beta_j \quad ; j = 2, \ldots\ldots, N \tag{24e}$$

Moreover, it should be emphasized that above integrations, may also be visualized as integration along the length of each sub-element of the truncation-element that is going to augment our model at the truncation boundary. In that context, interpolating functions in Eqs. (23a-e) leads to certain basic relations at the sub-element level. Assembling them for different sub-elements would lead to the following basic relations which are valid for the truncation-element as a whole.

$$-(2\bar{a}_1/\bar{c})\alpha_0\mathbf{L_I}\ddot{\mathbf{\Phi}}_0 + (2\bar{a}_0\bar{a}_1 + \beta_1)\mathbf{L_I}\ddot{\mathbf{\Phi}}_1 - \alpha_1\mathbf{L_I}\ddot{\mathbf{\Phi}}_2 + (2\bar{a}_1/\bar{c})\mathbf{Q_I}\dot{\mathbf{\Phi}}_0 + \mathbf{Q_I}\dot{\mathbf{\Phi}}_1 + \mathbf{Q_I}\dot{\mathbf{\Phi}}_2 + \\ (2\bar{a}_1/\bar{c})\mathbf{D_I}\mathbf{\Phi}_0 + \mathbf{D_I}\mathbf{\Phi}_1 + \mathbf{D_I}\mathbf{\Phi}_2 = \mathbf{0} \tag{25a}$$

$$-\bar{a}_j\alpha_{j-1}\mathbf{L_I}\ddot{\mathbf{\Phi}}_{j-1} + \gamma_j\mathbf{L_I}\ddot{\mathbf{\Phi}}_j - \bar{a}_{j-1}\alpha_j\mathbf{L_I}\ddot{\mathbf{\Phi}}_{j+1} + \bar{a}_j\mathbf{Q_I}\dot{\mathbf{\Phi}}_{j-1} + \xi_{j-1}\mathbf{Q_I}\dot{\mathbf{\Phi}}_j + \bar{a}_{j-1}\mathbf{Q_I}\dot{\mathbf{\Phi}}_{j+1} + \\ \bar{a}_j\mathbf{D_I}\mathbf{\Phi}_{j-1} + \xi_{j-1}\mathbf{D_I}\mathbf{\Phi}_j + \bar{a}_{j-1}\mathbf{D_I}\mathbf{\Phi}_{j+1} = \mathbf{0} \tag{25b}$$

$$-\alpha_N\mathbf{L_I}\ddot{\mathbf{\Phi}}_N + \beta_N\mathbf{L_I}\ddot{\mathbf{\Phi}}_{N+1} + \mathbf{Q_I}\dot{\mathbf{\Phi}}_N + 2\bar{a}_N\mathbf{L_I}\dot{\mathbf{\Psi}} + \mathbf{Q_I}\dot{\mathbf{\Phi}}_{N+1} + \mathbf{D_I}\mathbf{\Phi}_N + \mathbf{D_I}\mathbf{\Phi}_{N+1} = \mathbf{0} \tag{25c}$$

$$\bar{c}^2\mathbf{L_I}\ddot{\mathbf{\Phi}}_{N+1} + \bar{c}^2\mathbf{L_I}\ddot{\mathbf{\Phi}}_{N+2} + \mathbf{Q_I}\dot{\mathbf{\Phi}}_{N+1} + \mathbf{Q_I}\dot{\mathbf{\Phi}}_{N+2} - 2\bar{b}_1\mathbf{L_I}\dot{\mathbf{\Psi}} + (\bar{b}_1^2\mathbf{L_I} + \mathbf{D_I})\mathbf{\Phi}_{N+1} + (-\bar{b}_1^2\mathbf{L_I} + \mathbf{D_I})\mathbf{\Phi}_{N+2} = \mathbf{0} \tag{25d}$$

$$\bar{b}_{j+1}\bar{c}^2\mathbf{L_I}\ddot{\mathbf{\Phi}}_{N+j} + \eta_j\bar{c}^2\mathbf{L_I}\ddot{\mathbf{\Phi}}_{N+j+1} + \bar{b}_j\bar{c}^2\mathbf{L_I}\ddot{\mathbf{\Phi}}_{N+j+2} + \bar{b}_{j+1}\mathbf{Q_I}\dot{\mathbf{\Phi}}_{N+j} + \\ \eta_j\mathbf{Q_I}\dot{\mathbf{\Phi}}_{N+j+1} + \bar{b}_j\mathbf{Q_I}\dot{\mathbf{\Phi}}_{N+j+2} + (-\bar{b}_{j+1}\bar{b}_j^2\mathbf{L_I} + \bar{b}_{j+1}\mathbf{D_I})\mathbf{\Phi}_{N+j} + (\bar{b}_j\bar{b}_{j+1}\eta_j\mathbf{L_I} + \\ \eta_j\mathbf{D_I})\mathbf{\Phi}_{N+j+1} + (-\bar{b}_j\bar{b}_{j+1}^2\mathbf{L_I} + \bar{b}_j\mathbf{D_I})\mathbf{\Phi}_{N+j+2} = \mathbf{0} \tag{25e}$$

with the following sub-element matrix definitions

$$\mathbf{L_I^e} = \frac{1}{\rho}\int_y \mathbf{N}\mathbf{N}^{\mathrm{T}}dy \tag{26a}$$

$$\mathbf{Q_I} = \frac{q}{\rho}\tilde{\mathbf{I}}_I\,\tilde{\mathbf{I}}_I^{\mathrm{T}} \tag{26b}$$

$$\tilde{\mathbf{I}}_I = [1 \quad 0 \quad \ldots\ldots \quad 0 \quad 0]^{\mathrm{T}} \tag{26c}$$

$$\mathbf{D}_{\mathrm{I}}^{e} = \frac{1}{\rho} \int_{y} \mathbf{N}_{y} \mathbf{N}_{y}^{\mathrm{T}} dy \qquad (26d)$$

It is worthwhile to mention that subscript y in Eq. (26d) refers to partial derivative with respect to that coordinate. Furthermore, one should consider that last auxiliary vector must be a null vector based on requirement in relation (13d)

$$\mathbf{\Phi}_{N+M+1} = \mathbf{0} \qquad (27)$$

Apart from the above basic equations, certain other relations are required which are discussed in the next sub-sections.

3.2 Explicit form of R_I vector

The original aim for introducing truncation-element is to calculate $\mathbf{R}_{\mathrm{I}}$ term in relation (7). It was also explained in sub-section 2.4 about the procedure to calculate $\mathbf{R}_{\mathrm{I}}$ vector under general conditions. That task will be completed in present sub-section. For this purpose, one may substitute for $\partial_x \phi_0$ in Eq. (11) by employing Eq. (13a) which yields

$$\mathbf{R}_{\mathrm{I}}^{e} = \frac{1}{\rho} \int_{\Gamma_{I}^{e}} \mathbf{N} \left(-\bar{a}_0 \dot{\phi}_0 + \bar{c} \, \dot{\phi}_1 \right) d\Gamma^{e} \qquad (28)$$

This relation may also be visualized as being pertinent to each sub-element of the truncation-element. Interpolating function $\dot{\phi}_0$ and $\dot{\phi}_1$ by the help of shape functions, the above relation leads to

$$\mathbf{R}_{\mathrm{I}}^{e} = -\bar{a}_0 \, \mathbf{L}_{\mathrm{I}}^{e} \, \dot{\mathbf{\Phi}}_0^{e} + \bar{c} \, \mathbf{L}_{\mathrm{I}}^{e} \, \dot{\mathbf{\Phi}}_1^{e} \qquad (29)$$

Assembling these vectors results in

$$\mathbf{R}_{\mathrm{I}} = -\bar{a}_0 \, \mathbf{L}_{\mathrm{I}} \dot{\mathbf{\Phi}}_0 + \bar{c} \, \mathbf{L}_{\mathrm{I}} \dot{\mathbf{\Phi}}_1 \qquad (30)$$

It is recalled that ϕ_0 (equivalent to P^s) may be replaced through relation (9). Therefore, one would obtain

$$\mathbf{R}_{\mathrm{I}} + \bar{a}_0 \, \mathbf{L}_{\mathrm{I}} \left(\dot{\mathbf{P}} - \dot{\mathbf{P}}^i \right) - \bar{c} \, \mathbf{L}_{\mathrm{I}} \dot{\mathbf{\Phi}}_1 = \mathbf{0} \qquad (31)$$

3.3 Complementary relation to define incidence pressure wave vector

It was noticed that incidence pressure wave vector ($\mathbf{P}^i$) was introduced in Eq. (31). Therefore, this vector is also required to be defined through another complementary relation, which is discussed in this sub-section.

The incidence pressure wave function obeys the following governing equation

$$\bar{c}^2 \ddot{P}^i - \partial_y^2 P^i = 0 \qquad (32)$$

This is apparent since, it is a function independent of *x*-direction. Moreover, apart from top boundary condition ($P^i = 0$), it should satisfy the following boundary condition (recalling Eq. (3a))

$$\partial_y P^i = q \, \dot{P}^i - \rho a_g^y \qquad (33)$$

Solmaz Dehghanmarvasty and Vahid Lotfi

Let us now apply weighted residual approach to Eq. (32) by multiplying this relation by weighting function w and integrate it for each sub-element of truncation-element. This is written as

$$\frac{1}{\rho} \int_{\Gamma_{\bar{I}}^e} w \left(\bar{c}^2 \ddot{P}^i - \partial_y^2 P^i \right) d\Gamma^e = 0 \tag{34}$$

Interpolating w, P^i and $\ddot{P}^i$ in Eq. (34) by employing shape functions, it will lead to the following relation which is true for each sub-element

$$\bar{c}^2 \left(\frac{1}{\rho} \int_{\Gamma_{\bar{I}}^e} \mathbf{N}\mathbf{N}^{\mathrm{T}} d\Gamma^e \right) \ddot{\mathbf{P}}^{ie} + \left(\frac{1}{\rho} \int_{\Gamma_{\bar{I}}^e} \mathbf{N}_y \mathbf{N}_y^{\mathrm{T}} d\Gamma^e \right) \mathbf{P}^{ie} - \frac{1}{\rho} \partial_y P^i \Big|_{y_B}^{y_T} = \mathbf{0} \tag{35}$$

This relation may be rewritten by employing Eqs. (26a) and (26d)

$$\bar{c}^2 \, \mathbf{L}_{\mathrm{I}}^e \, \ddot{\mathbf{P}}^{ie} + \mathbf{D}_{\mathrm{I}}^e \, \mathbf{P}^{ie} - \frac{1}{\rho} \partial_y P^i \Big|_{y_B}^{y_T} = \mathbf{0} \tag{36}$$

Combining Eq. (36) for different sub-elements and taking into account Eq. (33), top surface condition ($P^i=0$), it would lead to the following relation

$$\bar{c}^2 \, \mathbf{L}_{\mathrm{I}} \, \ddot{\mathbf{P}}^i + \mathbf{D}_{\mathrm{I}} \, \mathbf{P}^i + \left[\frac{1}{\rho} \left(q \, \dot{P}^i - \rho a_g^y \right) \Big|_{y=0} \right] \check{\mathbf{I}}_{\mathrm{I}} = \mathbf{0} \tag{37}$$

It can also be written as

$$\bar{c}^2 \, \mathbf{L}_{\mathrm{I}} \, \ddot{\mathbf{P}}^i + \mathbf{Q}_{\mathrm{I}} \, \dot{\mathbf{P}}^i + \mathbf{D}_{\mathrm{I}} \, \mathbf{P}^i = -\mathbf{E}_{\mathrm{I}}^i \, \mathbf{a}_g \tag{38}$$

Where $\mathbf{Q}_{\mathrm{I}}$ and $\tilde{\mathbf{I}}_{\mathrm{I}}$ are defined in Eqs. (26b), (26c). Moreover, the following matrix definition is also employed:

$$\mathbf{E}_{\mathrm{I}}^i = [\mathbf{0} \quad -\tilde{\mathbf{I}}_{\mathrm{I}}] \tag{39}$$

3.4 Generalized matrices of H-W type truncation-element

Relation (38) was the last required matrix relation for applying H-W type truncation-element. Therefore, a complete equation set is obtained which comprise relations (31), (25a-e), and (38). It is again emphasized that last auxiliary vector in Eq. (25e) should also satisfy relation (27) which can be easily implemented in that equation. These relations are now written in the following compacted form

$$\mathbf{M}_{\mathrm{I}}\ddot{\mathbf{P}}_{\mathrm{I}} + \mathbf{C}_{\mathrm{I}}\dot{\mathbf{P}}_{\mathrm{I}} + \mathbf{K}_{\mathrm{I}}\mathbf{P}_{\mathrm{I}} + \widetilde{\mathbf{R}}_{\mathrm{I}} = \mathbf{F}_{\mathrm{I}} \tag{40}$$

It is worthwhile to define the following vectors employed in Eq. (40)

$$\mathbf{P}_{\mathrm{I}} = \begin{pmatrix} \mathbf{P}^{\mathrm{T}} & \mathbf{\Phi}_1^{\mathrm{T}} & \dots & \mathbf{\Phi}_N^{\mathrm{T}} & \mathbf{\Psi}^{\mathrm{T}} & \mathbf{\Phi}_{N+1}^{\mathrm{T}} & \dots & \mathbf{\Phi}_{N+M-1}^{\mathrm{T}} & \mathbf{P}^{i\mathrm{T}} \end{pmatrix}^{\mathrm{T}} \tag{41}$$

$$\widetilde{\mathbf{R}}_{\mathrm{I}} = \begin{pmatrix} \mathbf{R}_{\mathrm{I}}^{\mathrm{T}} & \mathbf{0} & \dots & \mathbf{0} & \mathbf{0} & \mathbf{0} & \dots & \mathbf{0} & \mathbf{0} \end{pmatrix}^{\mathrm{T}} \tag{42}$$

$$\mathbf{F}_{\mathrm{I}} = \begin{pmatrix} \mathbf{0} & \mathbf{0} & \dots & \mathbf{0} & \mathbf{0} & \mathbf{0} & \dots & \mathbf{0} & (-\mathbf{E}_{\mathrm{I}}^i \, \mathbf{a}_g)^{\mathrm{T}} \end{pmatrix}^{\mathrm{T}} \tag{43}$$

Moreover, details of generalized matrices (i.e., $\mathbf{M}_{\mathrm{I}}, \mathbf{C}_{\mathrm{I}}, \mathbf{K}_{\mathrm{I}}$) are provided in Tables 1-3 below:

Table 1 Explicit form of generalized matrix $\mathbf{M}_I$

	$\mathbf{P}^T$	Φ_1^T	Φ_{N-1}^T	Φ_N^T	Ψ^T	Φ_{N+1}^T	Φ_{N+2}^T	Φ_{N+3}^T	$\mathbf{P}^{iT}$
$\mathbf{P}$	0	0	0	0	0	0	0	0	0
Φ_1	$-(2\bar{a}_1/\bar{c})\alpha_0\mathbf{L}_I$	$(2\bar{a}_0\bar{a}_1+\beta_1)\mathbf{L}_I$	$-\alpha_1\mathbf{L}_I$	0	0	0	0	0	$(2\bar{a}_1/\bar{c})\alpha_0\mathbf{L}_I$
Φ_{N-1}	0	$-\bar{a}_{N-1}\alpha_{N-2}\mathbf{L}_I$	$\gamma_{N-1}\mathbf{L}_I$	$-\bar{a}_{N-2}\alpha_{N-1}\mathbf{L}_I$	0	0	0	0	0
Φ_N	0	0	$-\bar{a}_N\alpha_{N-1}\mathbf{L}_I$	$\gamma_N\mathbf{L}_I$	0	$-\bar{a}_{N-1}\alpha_N\mathbf{L}_I$	0	0	0
Ψ	0	0	0	$-\alpha_N\mathbf{L}_I$	0	$\beta_N\mathbf{L}_I$	0	0	0
Φ_{N+1}	0	0	0	0	0	$\bar{c}^2\mathbf{L}_I$	$\bar{c}^2\mathbf{L}_I$	0	0
Φ_{N+2}	0	0	0	0	0	$\bar{b}_2\bar{c}^2\mathbf{L}_I$	$\eta_1\bar{c}^2\mathbf{L}_I$	$\bar{b}_1\bar{c}^2\mathbf{L}_I$	0
Φ_{N+3}	0	0	0	0	0	0	$\bar{b}_3\bar{c}^2\mathbf{L}_I$	$\eta_2\bar{c}^2\mathbf{L}_I$	0
$\mathbf{P}^i$	0	0	0	0	0	0	0	0	$\bar{c}^2\mathbf{L}_I$

Table 2 Explicit form of generalized matrix $\mathbf{C}_I$

	$\mathbf{P}^T$	Φ_1^T	Φ_{N-1}^T	Φ_N^T	Ψ^T	Φ_{N+1}^T	Φ_{N+2}^T	Φ_{N+3}^T	$\mathbf{P}^{iT}$
$\mathbf{P}$	$\bar{a}_0\mathbf{L}_I$	$-\bar{c}\mathbf{L}_I$	0	0	0	0	0	0	$-\bar{a}_0\mathbf{L}_I$
Φ_1	$(2\bar{a}_1/\bar{c})\mathbf{Q}_I$	$\mathbf{Q}_I$	$\mathbf{Q}_I$	0	0	0	0	0	$-(2\bar{a}_1/\bar{c})\mathbf{Q}_I$
Φ_{N-1}	0	$\bar{a}_{N-1}\mathbf{Q}_I$	$\xi_{N-2}\mathbf{Q}_I$	$\bar{a}_{N-2}\mathbf{Q}_I$	0	0	0	0	0
Φ_N	0	0	$\bar{a}_N\mathbf{Q}_I$	$\xi_{N-1}\mathbf{Q}_I$	0	$\bar{a}_{N-1}\mathbf{Q}_I$	0	0	0
Ψ	0	0	0	$\mathbf{Q}_I$	$2\bar{a}_N\mathbf{L}_I$	$\mathbf{Q}_I$	0	0	0
Φ_{N+1}	0	0	0	0	0	$\mathbf{Q}_I$	$\mathbf{Q}_I$	0	0
Φ_{N+2}	0	0	0	0	0	$\bar{b}_2\mathbf{Q}_I$	$\eta_1\mathbf{Q}_I$	$\bar{b}_1\mathbf{Q}_I$	0
Φ_{N+3}	0	0	0	0	0	0	$\bar{b}_3\mathbf{Q}_I$	$\eta_2\mathbf{Q}_I$	0
$\mathbf{P}^i$	0	0	0	0	0	0	0	0	$\mathbf{Q}_I$

Table 3 Explicit form of generalized matrix $\mathbf{K}_I$

	$\mathbf{P}^T$	Φ_1^T	Φ_{N-1}^T	Φ_N^T	Ψ^T	Φ_{N+1}^T	Φ_{N+2}^T	Φ_{N+3}^T	$\mathbf{P}^{iT}$
$\mathbf{P}$	0	0	0	0	0	0	0	0	0
Φ_1	$(2\bar{a}_1/\bar{c})\mathbf{D}_I$	$\mathbf{D}_I$	$\mathbf{D}_I$	0	0	0	0	0	$-(2\bar{a}_1/\bar{c})\mathbf{D}_I$
Φ_{N-1}	0	$\bar{a}_{N-1}\mathbf{D}_I$	$\xi_{N-2}\mathbf{D}_I$	$\bar{a}_{N-2}\mathbf{D}_I$	0	0	0	0	0
Φ_N	0		$\bar{a}_N\mathbf{D}_I$	$\xi_{N-1}\mathbf{D}_I$	0	$\bar{a}_{N-1}\mathbf{D}_I$	0	0	0
Ψ	0	0	0	$\mathbf{D}_I$	0	$\mathbf{D}_I$	0	0	0
Φ_{N+1}	0	0	0	0	$-2\bar{b}_1\mathbf{L}_I$	$\bar{b}_1^2\mathbf{L}_I+\mathbf{D}_I$	$-\bar{b}_1^2\mathbf{L}_I+\mathbf{D}_I$	0	0
Φ_{N+2}	0	0	0	0	0	$-\bar{b}_2\bar{b}_1^2\mathbf{L}_I+\bar{b}_2\mathbf{D}_I$	$\bar{b}_1\bar{b}_2\eta_1\mathbf{L}_I+\eta_1\mathbf{D}_I$	$-\bar{b}_1\bar{b}_2^2\mathbf{L}_I+\bar{b}_1\mathbf{D}_I$	0
Φ_{N+3}	0	0	0	0	0	0	$-\bar{b}_3\bar{b}_2^2\mathbf{L}_I+\bar{b}_3\mathbf{D}_I$	$\bar{b}_2\bar{b}_3\eta_2\mathbf{L}_I+\eta_2\mathbf{D}_I$	0
$\mathbf{P}^i$	0	0	0	0	0	0	0	0	$\mathbf{D}_I$

4. Coupled equations of dam-reservoir system

The matrix equation of dam-reservoir system was already presented in sub-section 2.3 (i.e., Eq. (7)). Combining that equation with relation (40) would result in the coupled equation of dam-reservoir system in its final form

$$\begin{pmatrix} \mathbf{M} & \mathbf{0} \\ \overline{\mathbf{B}} & \mathbf{G} + \overline{\mathbf{M}}_\mathrm{I} \end{pmatrix} \begin{pmatrix} \ddot{\mathbf{r}} \\ \ddot{\overline{\mathbf{P}}} \end{pmatrix} + \begin{pmatrix} \mathbf{C} & \mathbf{0} \\ \mathbf{0} & q\overline{\mathbf{L}}_\mathrm{II} + \overline{\mathbf{C}}_\mathrm{I} \end{pmatrix} \begin{pmatrix} \dot{\mathbf{r}} \\ \dot{\overline{\mathbf{P}}} \end{pmatrix} + \begin{pmatrix} \mathbf{K} & -\overline{\mathbf{B}}^\mathrm{T} \\ \mathbf{0} & \overline{\mathbf{H}} + \overline{\mathbf{K}}_\mathrm{I} \end{pmatrix} \begin{pmatrix} \mathbf{r} \\ \overline{\mathbf{P}} \end{pmatrix} = \begin{pmatrix} -\widetilde{\mathbf{M}} \mathbf{J} \mathbf{a}_\mathrm{g} \\ -\widetilde{\overline{\mathbf{B}}} \mathbf{J} \mathbf{a}_\mathrm{g} + \overline{\mathbf{F}}_\mathrm{I} \end{pmatrix} \quad (44)$$

It is noted that vectors $\widetilde{\mathbf{R}}_\mathrm{I}$ and $-\mathbf{R}_\mathrm{I}$ cancel each other during this process. Furthermore, the bar sign over matrices emphasize that they are expanded by including additional zero terms for size consistency purposes. Additionally, the following definition for $\overline{\mathbf{P}}$ vector is utilized

$$\overline{\mathbf{P}} = \begin{pmatrix} \mathbf{P}^\mathrm{T} & \mathbf{\Phi}_1^\mathrm{T} & \dots & \mathbf{\Phi}_N^\mathrm{T} & \mathbf{\Psi}^\mathrm{T} & \mathbf{\Phi}_{N+1}^\mathrm{T} & \dots & \mathbf{\Phi}_{N+M-1}^\mathrm{T} & \mathbf{P}^{i\mathrm{T}} \end{pmatrix}^\mathrm{T} \quad (45)$$

It should be mentioned that difference between $\overline{\mathbf{P}}$ and $\mathbf{P}_\mathrm{I}$ vectors are merely the additional pressure degrees of freedom in $\mathbf{P}^\mathrm{T}$ part of the former vector (i.e., it includes all nodes in the reservoir domain except the ones at the impounding water surface (i.e., Γ_IV)). Moreover, it is now apparent based on Eq. (44) that the proposed approach is suitable for transient analysis. However, let us also simplify this relation for time harmonic analysis. Under these circumstances, one may write Eq. (44) as follows

$$\begin{pmatrix} -\omega^2 \mathbf{M} + (1 + 2\beta_d \mathrm{i})\mathbf{K} & -\overline{\mathbf{B}}^\mathrm{T} \\ -\omega^2 \overline{\mathbf{B}} & -\omega^2(\mathbf{G} + \overline{\mathbf{M}}_\mathrm{I}) + \mathrm{i}\omega(q\overline{\mathbf{L}}_\mathrm{II} + \overline{\mathbf{C}}_\mathrm{I}) + (\overline{\mathbf{H}} + \overline{\mathbf{K}}_\mathrm{I}) \end{pmatrix} \begin{pmatrix} \mathbf{r} \\ \overline{\mathbf{P}} \end{pmatrix} = \begin{pmatrix} -\widetilde{\mathbf{M}} \mathbf{J} \mathbf{a}_\mathrm{g} \\ -\widetilde{\overline{\mathbf{B}}} \mathbf{J} \mathbf{a}_\mathrm{g} + \overline{\mathbf{F}}_\mathrm{I} \end{pmatrix}$$
$$(46)$$

In this relation, it is assumed that the damping matrix of the dam is of hysteretic type. This means

$$\mathbf{C} = (2\beta_d/\omega)\mathbf{K} \quad (47)$$

5. Modeling and basic parameters

The introduced methodology is employed to analyze the Pine Flat dam-reservoir system. This particular dam was selected, because many researchers have analyzed it based on different approaches (Chopra *et al.* 1980, Feltrin *et al.* 1990, Lotfi 2002). The dam is 121.92 m high with the crest length of 560.83 m and it is located on the King's River near Fresno, California.

The details about modeling aspects such as discretization, basic parameters and the assumptions adopted are summarized in this section.

5.1 Models

Two-dimensional model of Pine Flat dam-reservoir system is considered on a rigid base. The dam is discretized by 40 isoparametric 8-node plane-solid finite elements in plane-stress state. As for the water domain, two strategies are adopted as explained below (Fig. 2):

For the FE-(FE-TE) method of analysis which is our main procedure, the reservoir near-field is discretized by fluid finite elements and the H-W high-order boundary condition is employed on the upstream truncation boundary. This latter task is actually carried out by utilizing a truncation-element at that boundary. The length of this near-field region is denoted by L and water depth is referred to as H. Two normalized reservoir length is considered herein. These are in particular; L/H=1 and 3. Herein, discretization corresponding to the lower length (i.e., L/H=1) is depicted in which 45 isoparametric 8-node plane-fluid finite elements are employed for modeling of the water region (Fig. 2). For the FE-(FE-HE) method of analysis, the reservoir domain is divided into two
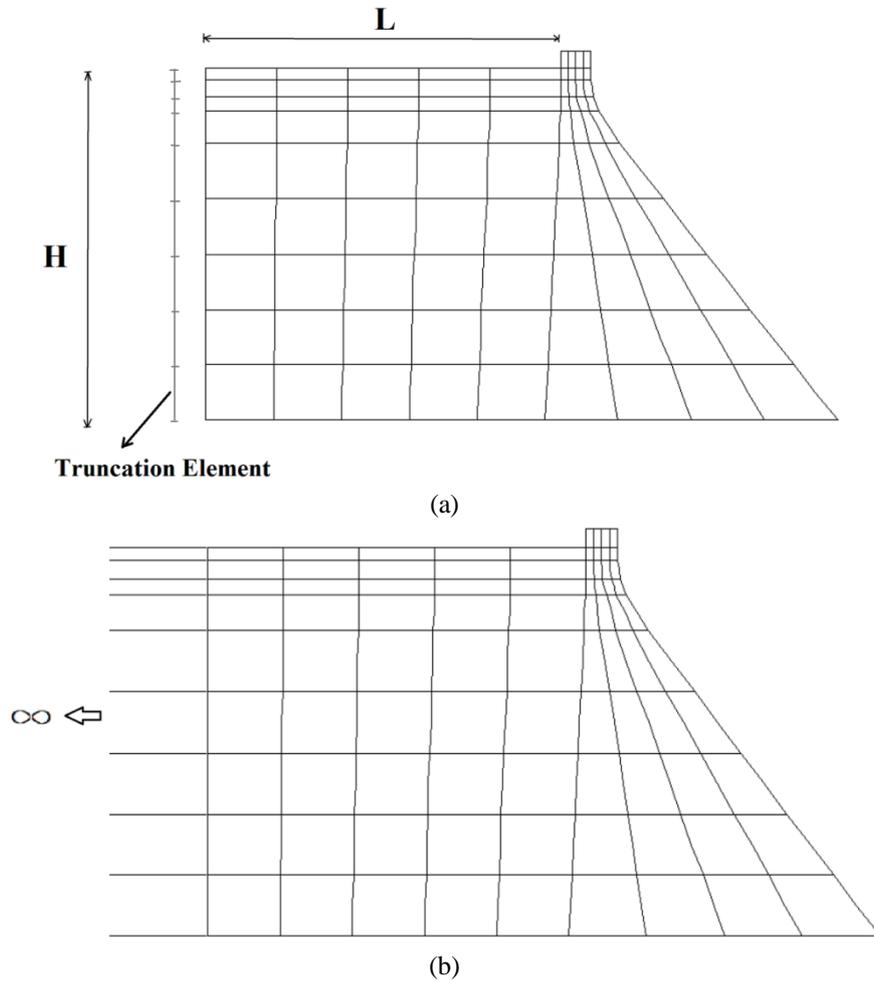
Fig. 2 The dam-reservoir discretization for L/H=1; (a) FE-(FE-TE) Model, (b) FE-(FE-HE) Model

regions. The near-field region (L/H=1) is discretized by fluid finite elements, and the far-field is treated by a fluid hyper-element (Fig. 2(b)). Of course, it should be emphasized that this option is merely utilized to obtain the exact solutions (Lotfi 2001b, Lotfi 2004). Moreover, it is well-known that the results are not sensitive in this case to the length of the reservoir near-field region or L/H value.

Furthermore, for each case two alternatives are considered which correspond to full reflective (i.e., $\alpha = 1$) and absorptive (i.e., $\alpha = 0.75$) reservoir bottom conditions.

The evaluation of H-W high order condition is initially carried out for time harmonic analysis. Subsequently, the investigation is performed for transient analysis by considering earthquake excitations.

5.2 Basic parameters

The concrete is assumed to be homogeneous and isotropic with the following basic properties:

Elastic modulus E_c = 22.75 GPa.

Poisson's ratio v_c = 0.20

Unit weight γ_c = 24.8 kN/m^3

Hysteretic damping factor $\beta_d = 0.05$ (Utilized for time harmonic analysis)

The water is taken as compressible, inviscid fluid, with weight density of 9.81 kN/m^3 and pressure wave velocity of 1440.0 m/s. The water level is considered at the height of 116.19 m above the base, similar to the reference (Chopra *et al.* 1980).

As mentioned, two different analysis types are carried out. These are time harmonic as well as transient type of analyses. For the former part, the hysteretic damping factor mentioned above is utilized. However, in the latter part., the Rayleigh damping matrix is applied and the corresponding coefficients are determined such that equivalent damping for frequencies close to the first and tenth modes of vibration corresponding to dam-reservoir system (i.e., $f_1 = 2.545$ Hz and $f_{10} = 8.690$ Hz) would be 5% of the critical damping.

5.3 Loading

For time harmonic analysis, the loading is merely ground motions. However, for transient analysis, it includes both static and dynamic type of loading. It should be mentioned that static loads (weight, hydrostatic pressures) are each visualized as being applied in one separate increment of time. Therefore, the same time step of 0.01 second, which is chosen in dynamic analysis, is also considered as time increment of static loads application. It is noted that time for static analysis is just a convenient tool for applying the load sequentially. However, it is obvious that inertia and damping effects are disregarded in the process. In this respect, the dead load is applied in one increment and hydrostatic pressures thereafter in another increment at negative range of time. At time zero, the actual dynamic analysis begins with the static displacements and stresses being applied as initial conditions. The dynamic excitation considered, is the S69E or vertical component of Taft earthquake records, which is applied in the horizontal or vertical directions separately, along with static loading mentioned. The time duration utilized, is 13 seconds in each case.

6. Results

The initial part of study focuses on the time harmonic analysis of Pine Flat dam-reservoir system. Subsequently, the transient type of analysis will be presented. It should be emphasized that a relatively high order of H-W truncation condition is utilized throughout this investigation (e.g., O5-5). It is also worthwhile to mention that all traveling-type parameters of H-W are taken equal ($a_j = 1$). Similarly, all evanescent-type parameters of H-W are also taken equal ($b_j = 11.0$). This latter value is selected by a calibration strategy mentioned for the analysis of gravity dams (Samii and Lotfi 2012).

6.1 Time harmonic analysis

It should be emphasized that all results presented herein, are obtained by the FE-(FE-TE) method discussed, under H-W type high-order absorbing condition applied on the truncation boundary. The only exception is for what are referred to as the exact responses. Those special

Horizontal Ground Motion   **Vertical Ground Motion**

(a)

Horizontal Ground Motion   **Vertical Ground Motion**

(b)
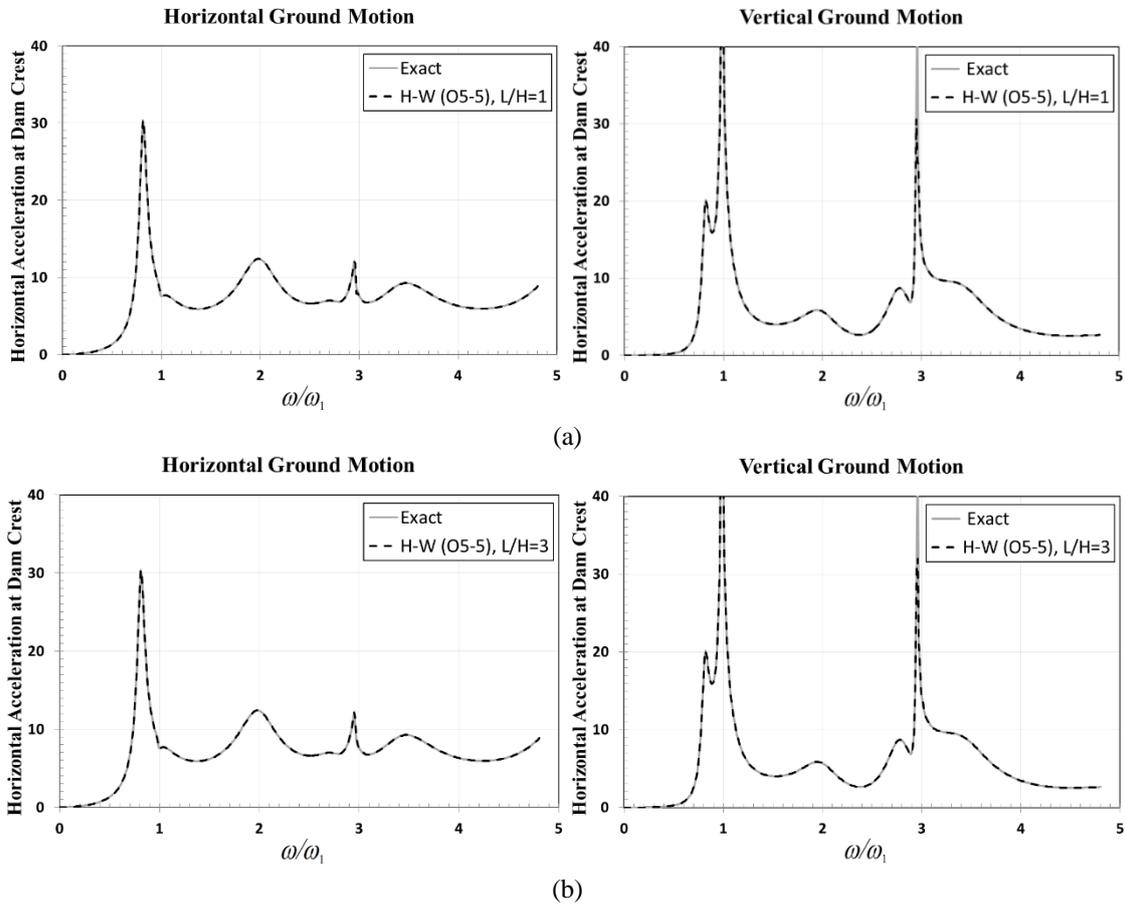
Fig. 3 Horizontal acceleration at dam crest due to horizontal and vertical ground motion for H-W (O5-5) condition and full reflective reservoir bottom condition (α=1.0); (a) L/H=1, (b) L/H=3

cases are carried out by the FE-(FE-HE) analysis technique (Lotfi 2004).

The study covers both full reflective and absorptive reservoir bottom condition (i.e., $\alpha = 1$ and 0.75). Moreover, responses are studied for both horizontal and vertical ground motions.

The transfer functions for the horizontal acceleration at dam crest with respect to horizontal or vertical ground acceleration are presented for full reflective and absorptive reservoir bottom conditions in Figs. 3 and 4, respectively. It is noted that response in each case is plotted versus the dimensionless frequency. The normalization of excitation frequency is carried out with respect to ω_1, which is defined as the natural frequency of the dam with an empty reservoir on rigid foundation. Moreover, it is noticed that all cases are compared with its corresponding exact response.

Let us first consider the full reflective reservoir bottom condition (Fig. 3). It is noted that response in each case matches perfectly against the corresponding exact response throughout considered frequency range. This is true for both low and high normalized reservoir lengths (i.e., L/H=1 and 3), as well as both horizontal and vertical ground motions. It is such that it is hardly distinguishable from the exact response for all cases. Similar trend is also observed for the
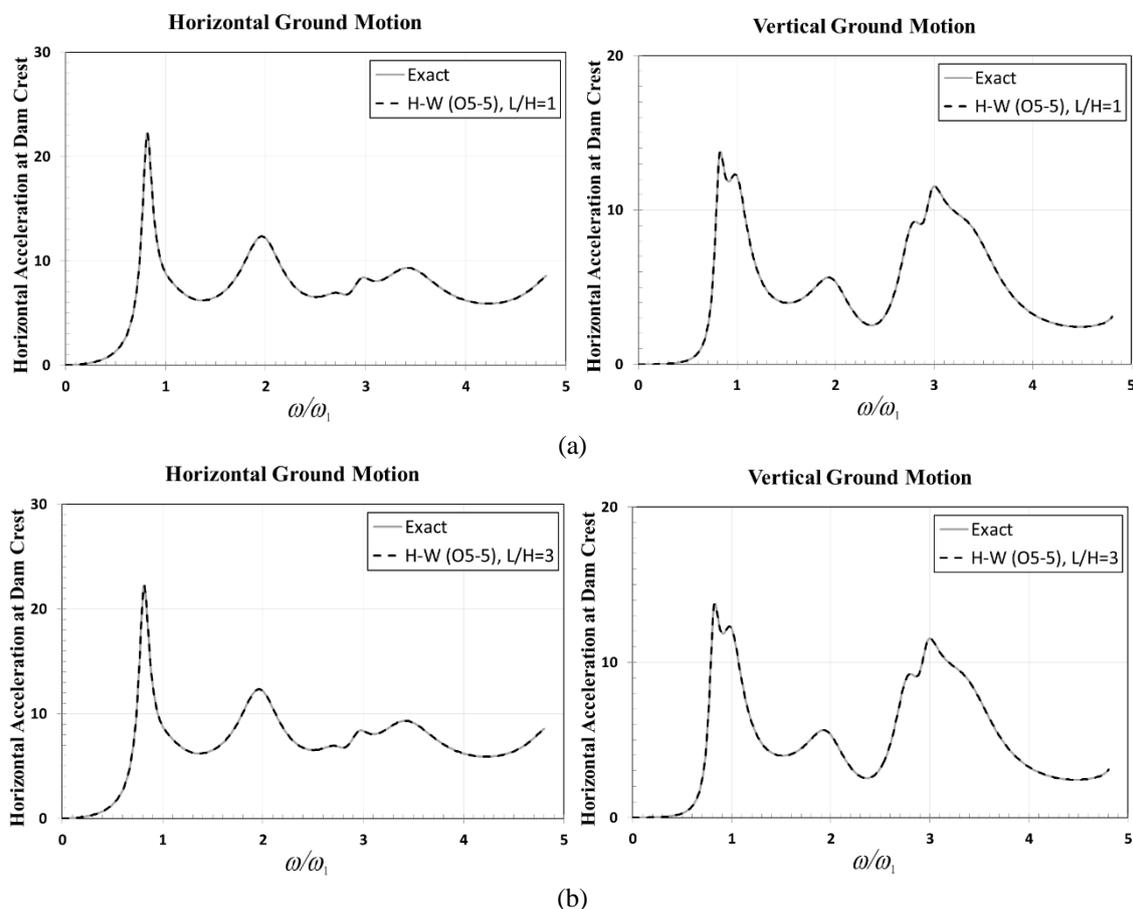
Fig. 4 Horizontal acceleration at dam crest due to horizontal and vertical ground motion for H-W (O5-5) condition and absorptive reservoir bottom condition (α=0.75); (a) L/H=1, (b) L/H=3

absorptive reservoir bottom condition (Fig. 4). This means that truncation element based on high order of H-W condition (e.g., O5-5) is working perfectly and produces similar results to exact responses for time harmonic analysis for the vast frequency range considered. In other words, the results are not sensitive to the normalized reservoir length values. Therefore, one expects that similar observation is reached when the transient analysis is carried that. If this is verified, one could claim that transient analysis leads practically to exact results (in numerical sense) when one is employing high order H-W truncation element. This will be discussed in the next sub-section.

6.2 Transient analysis

It is worthwhile to emphasize that all results presented in this sub-section are obtained by the FE-(FE-TE) method discussed, under high order of H-W condition (e.g., O5-5) applied on the truncation boundary. This is due to the fact FE-(FE-HE) approach utilized in previous sub-section (referred to as exact method) is merely applicable for frequency domain analysis. Therefore, the main task herein is to investigate the sensitivity of response for normalized reservoir length. This
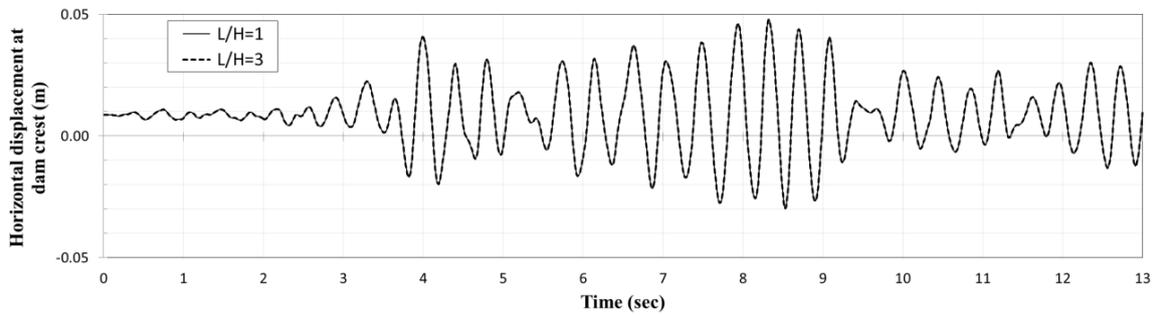
Fig. 5 Comparison of horizontal displacement at dam crest due to horizontal ground motion for L/H=1 and 3 (Full reflective reservoir bottom condition (α=1.0))
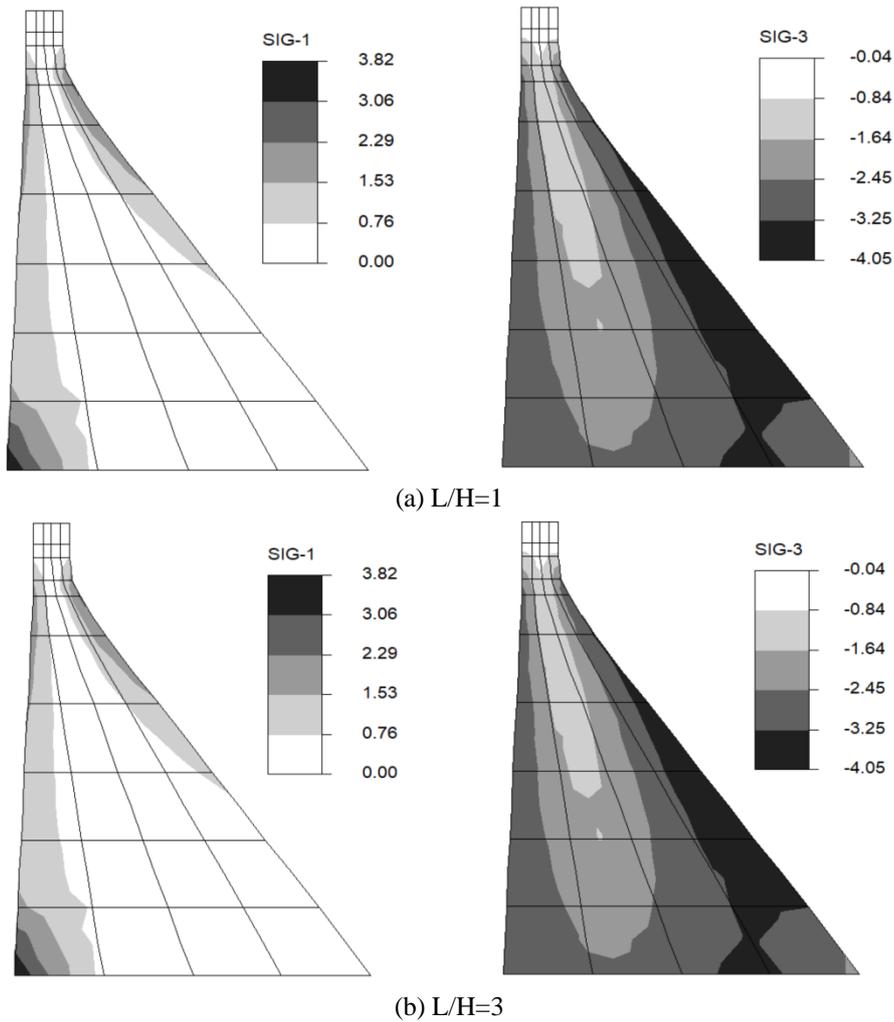
(a) L/H=1

(b) L/H=3

Fig. 6 Comparison of envelope of principal stresses due to horizontal excitation (Full reflective reservoir bottom condition (α=1.0)); (a) L/H=1, (b) L/H=3
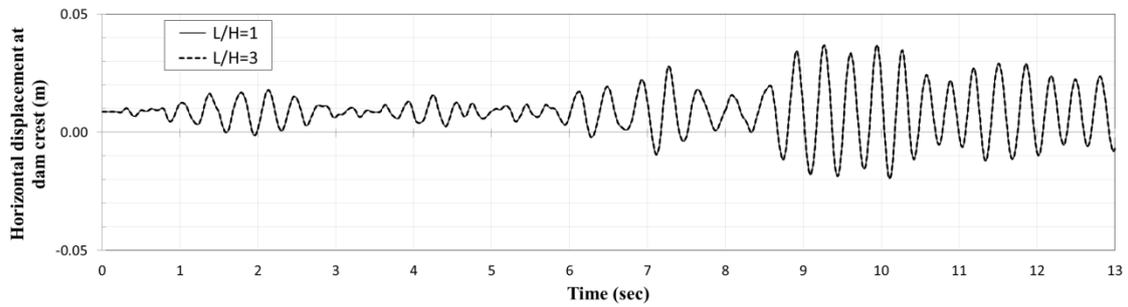
Fig. 7 Comparison of horizontal displacement at dam crest due to vertical ground motion for L/H=1 and 3 (Full reflective reservoir bottom condition (α=1.0))
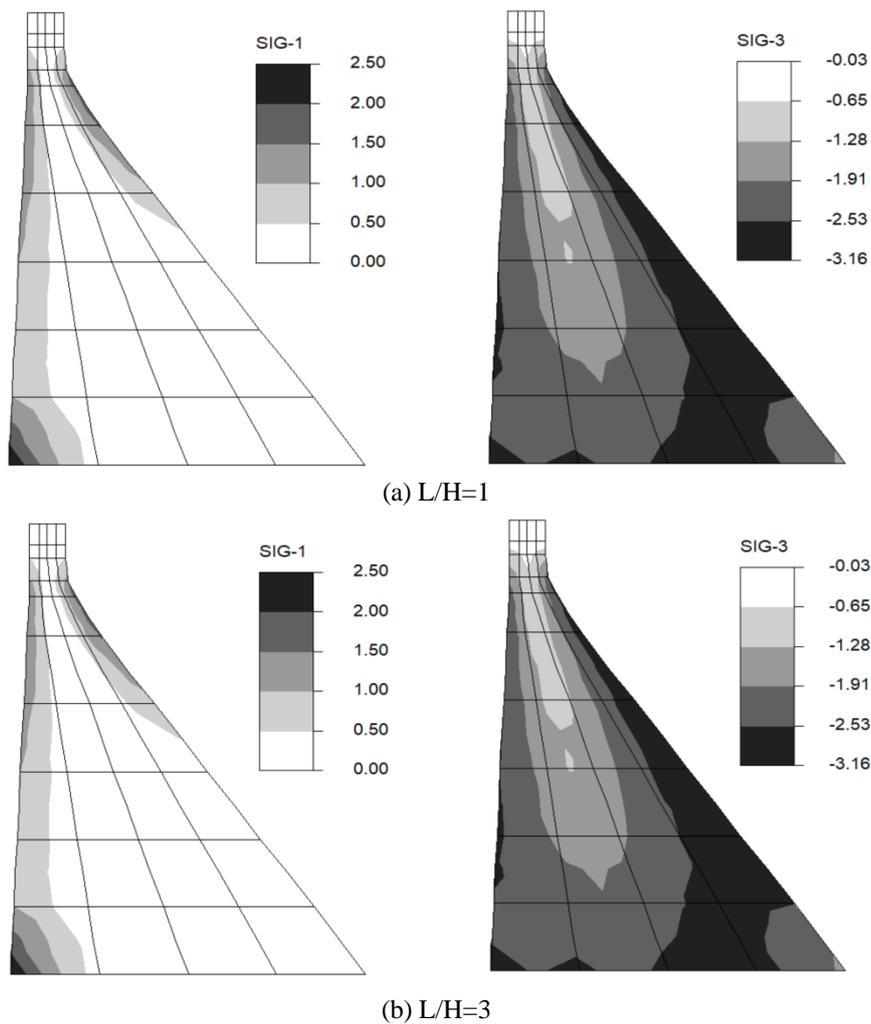
(a) L/H=1

(b) L/H=3

Fig. 8 Comparison of envelope of principal stresses due to vertical excitation (Full reflective reservoir bottom condition (α=1.0)); (a) L/H=1, (b) L/H=3
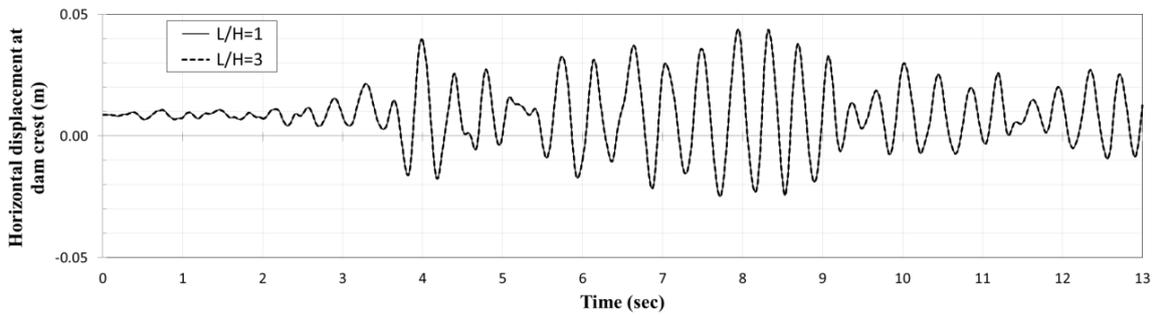
Fig. 9 Comparison of horizontal displacement at dam crest due to horizontal ground motion for L/H=1 and 3 (Absorptive reservoir bottom condition (α=0.75))
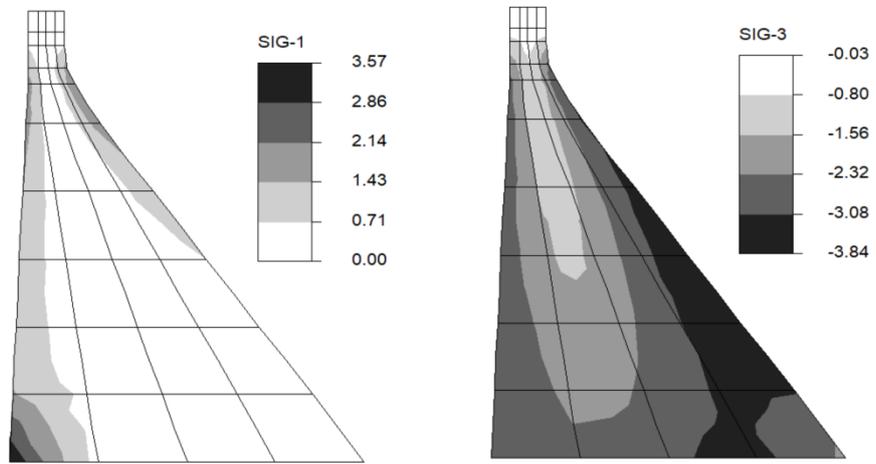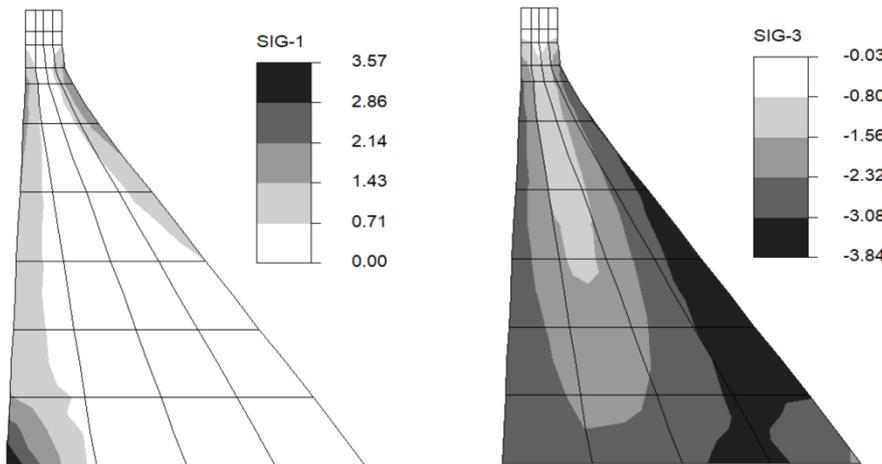
(a) L/H=1

(b) L/H=3

Fig. 10 Comparison of envelope of principal stresses due to horizontal excitation (Absorptive reservoir bottom condition (*α*=0.75)); (a) L/H=1, (b) L/H=3
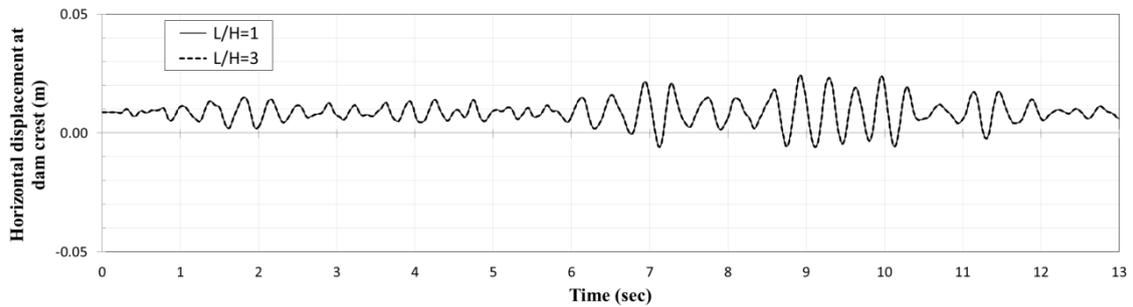
Fig. 11 Comparison of horizontal displacement at dam crest due to vertical ground motion for L/H=1 and 3 (Absorptive reservoir bottom condition (α=0.75))
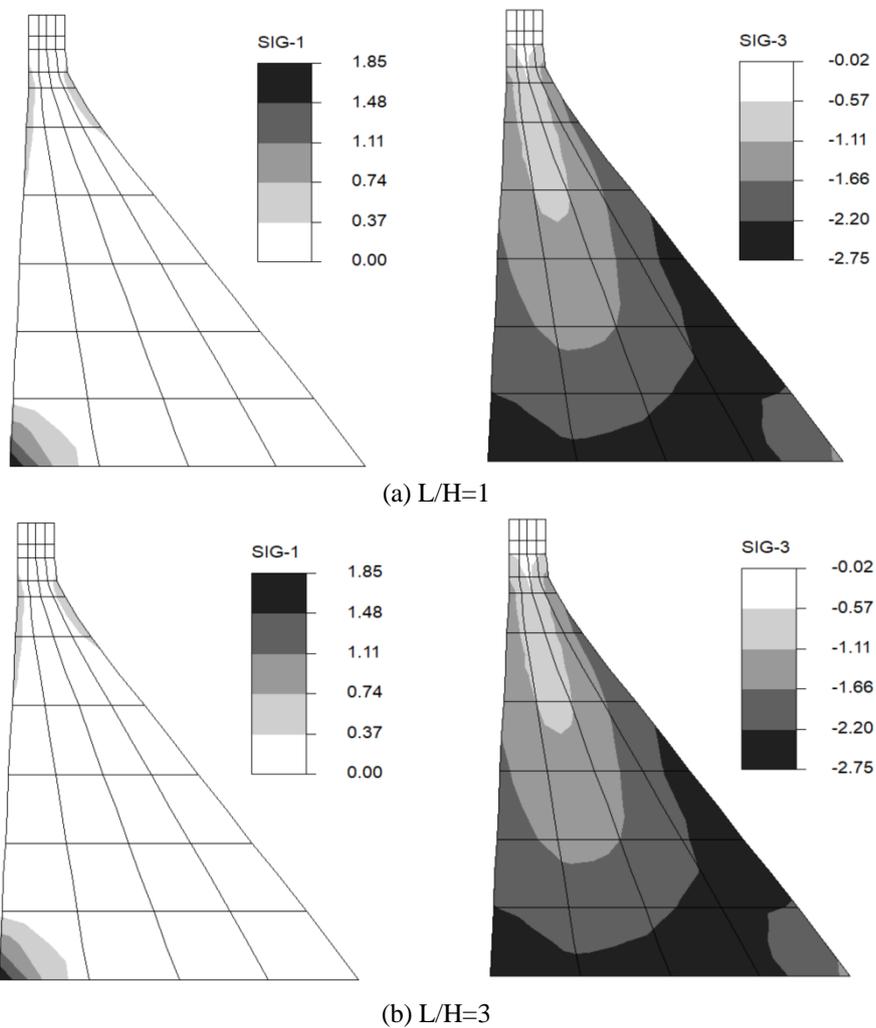
(a) L/H=1

(b) L/H=3

Fig. 12 Comparison of envelope of principal stresses due to vertical excitation (Absorptive reservoir bottom condition (α=0.75)); (a) L/H=1, (b) L/H=3

should be controlled for horizontal and vertical excitations, as well as both full reflective and absorptive reservoir bottom condition. In this respect, the dynamic excitation considered, is the S69E or vertical component of Taft earthquake records, which is applied in the horizontal or vertical directions separately, along with static loading mentioned.

Let us first consider the responses under full reflective reservoir bottom condition and horizontal excitation. At first, the time history of horizontal displacement at dam crest is compared for low and high normalized reservoir length cases (L/H=1 and 3) under these circumstances (Fig. 5). It is noted that response matches perfectly well for these two cases. Moreover, envelopes of principal stresses are presented in Fig. 6. It is again noted that perfect agreement exist between the patterns and their maximum and minimum values of the plotted contours.

Similar observations are also noticed for vertical excitation (Figs. 7 and 8). Moreover, this is also true similarly for absorptive reservoir bottom condition under both horizontal (Figs. 9 and 10) and vertical excitations (Figs. 11 and 12). Therefore, it can be claimed that transient analysis leads practically to exact results (in numerical sense) when one is employing high order H-W truncation element. In other words, the results are not sensitive to reservoir normalized length under these circumstances.

6.3 Influence of time increment in transient analysis

It is also interesting to evaluate the effect of time increment on transient analysis. It should be emphasized that all results mentioned in previous section was carried out with time increment $\Delta t = 0.01$ second. For this aim, an additional series of analysis were executed with $\Delta t = 0.005$ second. These were carried out under full reflective reservoir bottom condition and horizontal excitation. The results are presented in Figs. 13 and 14.

At first, the time history of horizontal displacement at dam crest is compared for low and high normalized reservoir length cases (L/H=1 and 3) under these circumstances (Fig. 13). It is noted that response matches perfectly well for these two cases. Moreover, they are practically the same as previous result (corresponding to L/H=1 and $\Delta t = 0.01$ second) which is included in that graph for reference purposes. It is noted that minor differences are not even easily distinguishable. Subsequently, envelopes of principal stresses are presented for both low and high normalized reservoir length cases (L/H=1 and 3) under these circumstances (Fig. 14). It is again noted that perfect agreement exist between the patterns and their maximum and minimum values of the plotted contours. Of course, it is slightly different from previous results (Figs. 14 vs 6). For
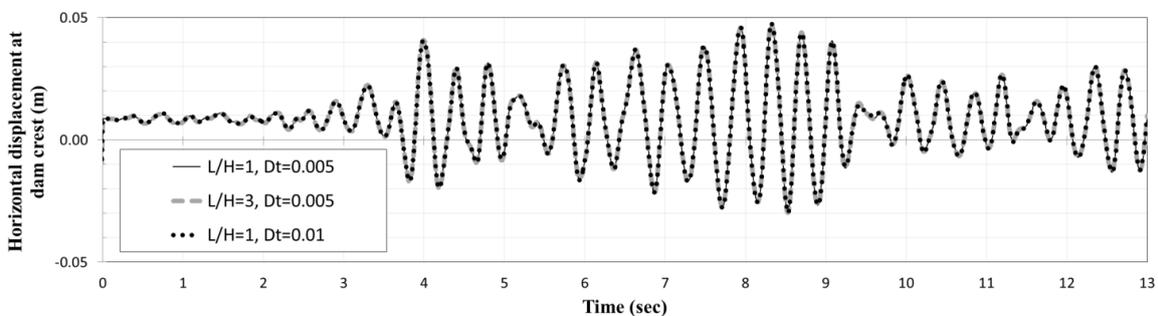
Fig. 13 Comparison of horizontal displacement at dam crest due to horizontal ground motion for L/H=1 and 3 (Full reflective reservoir bottom condition (α=1.0)), $\Delta t = 0.005$ sec.
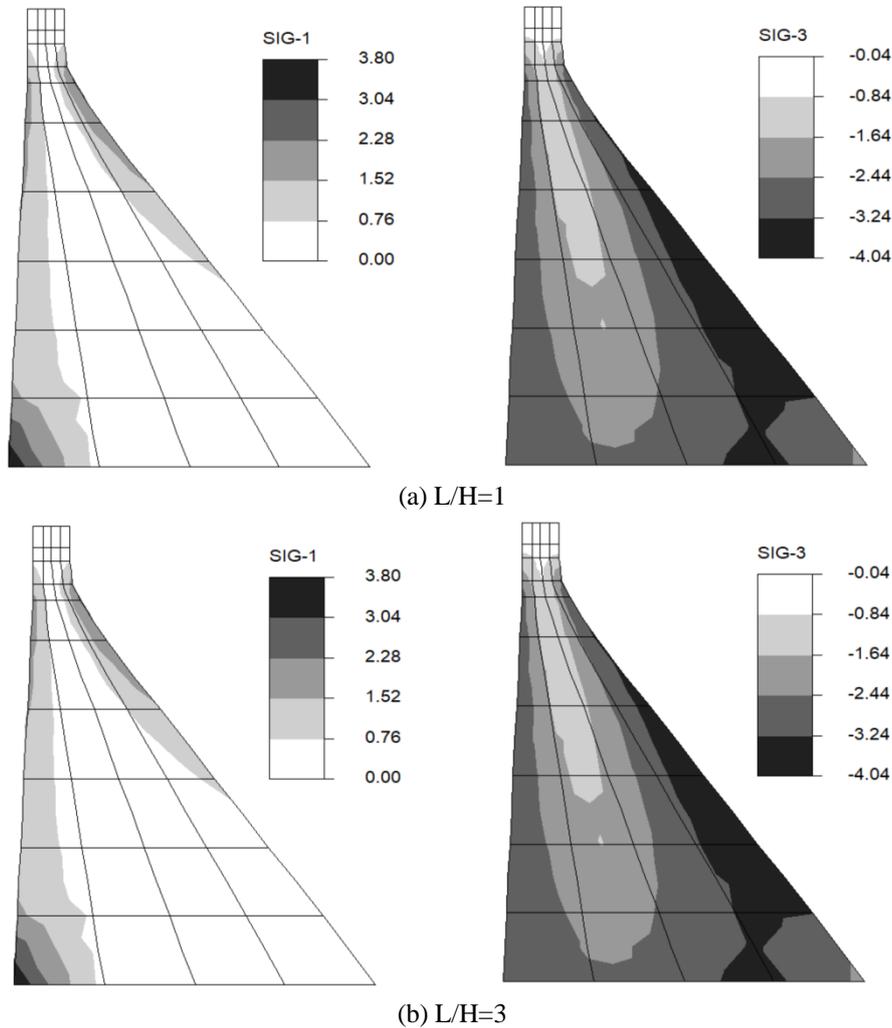
(a) L/H=1

(b) L/H=3

Fig. 14 Comparison of envelope of principal stresses due to horizontal excitation (Full reflective reservoir bottom condition (α=1.0)), $\Delta t = 0.005$ sec.; (a) L/H=1, (b) L/H=3

instance, it is noted that maximum tensile stress difference is about 0.5% (3.80 MPa vs 3.82 MPa). It is interesting that even with lower value of time increment, the results are not sensitive to normalized reservoir length value and the analysis approach leads to accurate results.

7. Conclusions

The formulation based on FE-(FE-TE) procedure, was examined for dynamic analysis of a realistic concrete gravity dam-reservoir system. The core of the method is based on utilizing a truncation-element at the U/S truncation boundary of the reservoir near-field domain and excluding far-field region of the reservoir. This truncation-element is formulated based on the

high-order condition of H-W type applied at that boundary. A special purpose finite element program (Lotfi 2001a) was enhanced for this investigation. Thereafter, the response of Pine Flat dam-reservoir system was studied due to horizontal and vertical ground motions for two types of reservoir bottom conditions of full reflective (i.e., $\alpha = 1$) and absorptive (i.e., $\alpha = 0.75$). It should be emphasized that study was carried out under high order of H-W condition (e.g., O5-5) applied on the truncation boundary.

The initial part of study was focused on the time harmonic analysis. In this part, it was possible to compare the transfer functions against corresponding responses obtained by FE-(FE-HE) approach (referred to as exact method). Subsequently, the transient analysis is carried out. In this part, it is only possible to compare the results for low and high normalized reservoir length cases (L/H=1 and 3). Therefore, the sensitivity of results is controlled due to normalized reservoir length values.

Overall, the main conclusions obtained by the present study can be listed as follows:
• High orders of H-W condition, such as O5-5 considered herein, generate highly accurate responses for both possible excitations under both types of full reflective and absorptive reservoir bottom conditions. It is such that transfer functions are hardly distinguishable from corresponding exact responses obtained through FE-(FE-HE) approach in time harmonic analyses. This is controlled for both low and high normalized reservoir length cases (L/H=1 and 3).
• In transient analysis, the time history of horizontal displacement at dam crest is compared for low and high normalized reservoir length cases (L/H=1 and 3). It is noted that response matches perfectly well for these two cases. Moreover, envelopes of principal stresses are compared which reveals that perfect agreement exist between the patterns and their maximum and minimum values of the plotted contours. These observations are noticed for both horizontal and vertical excitations as well as both full reflective and absorptive reservoir bottom condition. Therefore, it can be claimed that transient analysis leads practically to exact results (in numerical sense) when one is employing high order H-W truncation element. In other words, the results are not sensitive to reservoir normalized length under these circumstances.

References

Basu, U. and Chopra, A.K. (2003), "Perfectly matched layers for time-harmonic elastodynamics of unbounded domains: Theory and finite-element implementation", *Comput. Meth. Appl. Mech. Eng.*, **192**(11-12), 1337-1375. https://doi.org/10.1016/S0045-7825(02)00642-4.

Berenger, J.P. (1994), "A perfectly matched layer for the absorption of electromagnetic waves", *J. Comput. Phys.*, **114**(2), 185-200. https://doi.org/10.1006/jcph.1994.1159.

Chew, W.C. and Weedon, W.H. (1994), "A 3D perfectly matched medium from modified Maxwell's equations with stretched coordinates", *Microw. Opt. Techn. Let.*, **7**(13), 599-604. https://doi.org/10.1002/mop.4650071304.

Chopra, A.K. (1967), "Hydrodynamic pressure on dams during earthquake", *J. Eng. Mech.*, **93**, 205-223. https://doi.org/10.1061/JMCEA3.0000915.

Chopra, A.K., Chakrabarti, P. and Gupta, S. (1980), "Earthquake response of concrete gravity dams including hydrodynamic and foundation interaction effects", Report No. EERC-80/01, University of California, Berkeley.

Dehghanmarvasty, S. and Lotfi, V. (2022), "Accuracy of Hagstrom-Warburton high-order truncation boundary condition in time harmonic analysis of concrete gravity dam-reservoir systems", *Submitted to*

the Iranian Journal of Science and Technology, Transactions of Civil Engineering.

Dehghanmarvasty, S. and Lotfi, V. (2023), "Application of G-N high-order boundary condition on time harmonic analysis of concrete gravity dam-reservoir systems", *Eng. Comput.*, **40**(2), 313-334. https://doi.org/10.1108/EC-06-2022-0401.

Feltrin, G., Wepf, D. and Bachmann, H. (1991). "Seismic cracking of concrete gravity dams", *International Conference on Earthquake Resistant Construction and Design*, 371-380.

Fenves, G. and Chopra, A.K. (1985), "Effects of reservoir bottom absorption and dam-water-foundation interaction on frequency response functions for concrete gravity dams", *Earthq. Eng. Struct. Dyn.*, **13**, 13-31. https://doi.org/10.1002/eqe.4290130104.

Givoli, D. and Neta, B. (2003), "High order non-reflecting boundary scheme for time-dependent waves", *J. Comput. Phys.*, **186**(1), 24-46. https://doi.org/10.1016/S0021-9991(03)00005-6.

Givoli, D., Hagstrom, T., and Patlashenko, I. (2006), "Finite-element formulation with high-order absorbing conditions for time-dependent waves", *Comput. Meth. Appl. Mech. Eng.*, **195**(29-32), 3666-3690. https://doi.org/10.1016/j.cma.2005.01.021.

Hadzalic, E., Ibrahimbegovic, A. and Dolarevic, S. (2018), "Fluid-structure interaction system predicting both internal pore pressure and outside hydrodynamic pressure", *Couple. Syst. Mech.*, **7**(6), 649-668. https://doi.org/10.12989/csm.2018.7.6.649.

Hadzalic, E., Ibrahimbegovic, A. and Dolarevic, S. (2019), "Theoretical formulation and seamless discrete approximation for localized failure of saturated poro-plastic structure interacting with reservoir", *Comput. Struct.*, **214**, 73-93. https://doi.org/10.1016/j.compstruc.2019.01.003.

Hagstrom, T. and Warburton, T. (2004), "A new auxiliary variable formulation of high order local radiation boundary condition: corner compatibility conditions and extensions to first-order systems", *Wave Motion*, **39**(4), 327-338. https://doi.org/10.1016/j.wavemoti.2003.12.007.

Hagstrom, T., Mar-Or, A. and Givoli, D. (2008), "High-order local absorbing conditions for the wave equation: extensions and improvements", *J. Comput. Phys.*, **227**, 3322-3357. https://doi.org/10.1016/j.jcp.2007.11.040.

Hall, J.F. and Chopra, A.K. (1982), "Two-dimensional dynamic analysis of concrete gravity and embankment dams including hydrodynamic effects", *Earthq. Eng. Struct. Dyn.*, **10**(2), 305-332. https://doi.org/10.1002/eqe.4290100211.

Higdon, R.L. (1986), "Absorbing boundary conditions for difference approximations to the multi-dimensional wave equation", *Math. Comput.*, **47**(176), 437-459. https://doi.org/10.1090/S0025-5718-1986-0856696-4.

Jafari, M. and Lotfi, V. (2017), "Dynamic analysis of concrete gravity dam-reservoir systems by Wavenumber approach for the general reservoir base condition", *Scientia Iranica*, **25**(6), 3054-3065.

Jiong, L., Jian-wei, M. and Hui-zhu, Y (2009), "The study of perfectly matched layer absorbing boundaries for SH wave fields", *Appl. Geophys.*, **6**(3), 267-274. https://doi.org/10.1007/s11770-009-0023-0.

Karabulut, M. and Kartal, M.E. (2018), "Seismic analysis of concrete arch dams considering hydrodynamic effect using Westergaard approach", *Sakarya Univ. J. Sci.*, **23**(2), 149-161. https://doi.org/10.16984/saufenbilder.394266.

Khazaee, A. and Lotfi, V. (2014a), "Application of perfectly matched layers in the transient analysis of dam-reservoir systems", *J. Soil Dyn. Earthq. Eng.*, **60**(1), 51-68. https://doi.org/10.1016/j.soildyn.2014.01.005.

Khazaee, A. and Lotfi, V. (2014b), "Time harmonic analysis of dam-foundation systems by perfectly matched layers", *Struct. Eng. Mech.*, **50**(3), 349-364. https://doi.org/10.12989/sem.2014.50.3.349.

Kim, S. and Pasciak, J.E. (2010), "Analysis of a Cartesian PML approximation to acoustic scattering problems in R2", *J. Math. Anal. Appl.*, **370**(1), 168-186. https://doi.org/10.1016/j.jmaa.2010.05.006.

Lokke, A. and Chopra, A.K. (2017), "Direct finite element method for nonlinear analysis of semi-unbounded dam-water-foundation rock systems", *Earthq. Eng. Struct. Dyn.*, **46**(8), 1267-1285. https://doi.org/10.1002/eqe.2855.

Lokke, A. and Chopra, A.K. (2018), "Direct finite element method for nonlinear earthquake analysis of 3-dimensional semi-unbounded dam-water-foundation rock systems", *Earthq. Eng. Struct. Dyn.*, **47**(5), 1309-1328. https://doi.org/10.1002/eqe.3019.

Lotfi, V. (2001a), "MAP-76: A program for analysis of concrete dams", Department of Civil & Environmental Engineering, Amirkabir University of Technology, Tehran, Iran.

Lotfi, V. (2001b), "Frequency domain analysis of gravity dams including hydrodynamic effects", *Dam Eng.*, **12**(1), 33-53.

Lotfi, V. (2002), "Seismic analysis of concrete dams using the pseudo-symmetric technique", *Dam Eng.*, **13**(2), 119-145.

Lotfi, V. (2004), "Direct frequency domain analysis of concrete arch dams based on FE-(FE-HE)-BE technique", *Comput. Concrete*, **1**(3), 285-302. https://doi.org/10.12989/cac.2004.1.3.285.

Lotfi, V. (2017), "Dynamic analysis of concrete gravity dam-reservoir systems by Wavenumber approach for the general reservoir base condition and ground excitation", *Dam Eng.*, **27**(3), 33-57.

Lotfi, V. and Lotfi, A. (2022), "Time harmonic analysis of concrete arch dam-reservoir systems by utilizing GN high-order truncation condition", *Scientia Iranica*, **29**(6), 2825-2836.

Lotfi, V. and Omidi, O. (2012), "Dynamic analysis of Koyna dam using three-dimensional plastic-damage modeling", *Dam Eng.*, **22**(3), 197-226.

Lotfi, V. and Samii, A. (2012), "Dynamic analysis of concrete gravity dam-reservoir systems by wavenumber approach in the frequency domain", *Earthq. Struct.*, **3**(3), 533-548. https://doi.org/10.12989/eas.2012.3.3.533.

Lotfi, V. and Zenz, G. (2016), "Transient analysis of concrete gravity dam-reservoir systems by Wavenumber-TD approach", *Soil Dyn. Earthq. Eng.*, **90**(1), 313-326. https://doi.org/10.1016/j.soildyn.2016.08.026.

Lotfi, V. and Zenz, G. (2018), "Application of Wavenumber-TD approach for time harmonic analysis of concrete arch dam-reservoir systems", *Couple. Syst. Mech.*, **7**(3), 353-371. https://doi.org/10.12989/csm.2018.7.3.353.

Rabinovich, D., Givoli, D., Bielak, J. and Hagstrom, T. (2011), "A finite element scheme with a high order absorbing boundary condition for elastodynamics", *Comput. Meth. Appl. Mech.*, **200**, 2048-2066. https://doi.org/10.1016/j.cma.2011.03.006.

Samii, A. and Lotfi, V. (2012), "High-order adjustable boundary condition for absorbing evanescent modes of waveguides and its application in coupled fluid-structure analysis", *Wave Motion*, **49**(2), 238-257. https://doi.org/10.1016/j.wavemoti.2011.10.001.

Sharma, V., Fujisawa, K. and Murakami, A. (2019), "Space-time finite element procedure with block-iterative algorithm for dam-reservoir-soil interaction during earthquake loading", *Int. J. Numer. Meth. Eng.*, **120**(3), 263-282. https://doi.org/10.1002/nme.6134.

Sommerfeld, A. (1949), *Partial Differential Equations in Physics*, Academic Press, NY.

Waas, G. (1972), "Linear two-dimensional analysis of soil dynamics problems in semi-infinite layered media", Ph.D. Dissertation, University of California, Berkeley, California.

Zhen, Q., Minghui, L., Xiaodong, Z., Yao, Y., Cai, Z. and Jianyong, S. (2009), "The implementation of an improved NPML absorbing boundary condition in elastic wave modeling", *Appl. Geophys.*, **6**(2), 113-121. https://doi.org/10.1007/s11770-009-0012-3.

Zienkiewicz, O.C., Taylor, R.L. and Zhu, J.Z. (2013), *The Finite Element Method*, Butterworth-Heinemann.

AI